

THESIS

A RAPID, POINT OF NEED OPEN COW TEST

Submitted by

Jacy Mendez

Department of Chemical and Biological Engineering

In partial fulfillment of the requirements

For the Degree of Master of Science

Colorado State University

Fort Collins, Colorado

Fall 2023

Master's Committee:

Advisor: David Dandy

Chuck Henry

Travis Bailey

Thomas Hansen

Copyright by Jacy Ciara Mendez 2023

All Rights Reserved

## ABSTRACT

### A RAPID, POINT OF NEED OPEN COW TEST

In the dairy industry, maintaining non-pregnant (open) cows is expensive, and may require multiple rounds of artificial insemination (AI) for a cow to become pregnant. There is a need for early pregnancy detection in dairy cows, which allows the use of protocols such as prostaglandin F<sub>2</sub>-alpha (PGF) and gonadotropin releasing hormone (GnRH) to prepare a cow for another round of breeding via AI, with an emphasis on reduced time between each breeding attempt. The current gold standard method for confirming pregnancy in cows is a rectally-guided ultrasound at day 32 after AI. Interferon-tau (IFNT) is a biomarker that can be detected during days 7-28 of pregnancy in cattle, and is expressed by the cow conceptus. The goal of this work was to develop a cow-side test utilizing IFNT as the biomarker for early cattle pregnancy detection. A lateral flow assay (LFA) was chosen and investigated due to its simplicity and ease of use, but was later adapted to utilize the enzymatic oxidation of 3,3',5,5' – Tetramethylbenzidine to amplify the signal in the test line. C-reactive protein was used to develop protocols for aspects of device development involving nitrocellulose, including antibody striping, blocking, and nitrocellulose selection. These protocols were then utilized as optimization of the lateral flow assay was conducted. The resulting LFA has a limit of detection (LOD) of 10 µg/mL, with an LOD of 100 ng/mL in a half-strip format, with some limitations imposed by false positives. This work provides a novel method of detection for pregnancy in cattle and with further development, has the potential for use by dairy farmers in their respective industry.

## ACKNOWLEDGEMENTS

I am thankful for the guidance and support provided by my supervisor, Dr. David Dandy, during my research. Additionally, I appreciate the assistance of my collaborator and collaborator/committee member, Jeanette Bishop and Dr. Thomas Hansen. I would also like to thank my other committee members, Dr. Chuck Henry and Dr. Travis Bailey, for their helpful comments. Finally, I am extremely grateful for my husband, Rene, for supporting me unconditionally during this experience.

## TABLE OF CONTENTS

ABSTRACT.....	ii
ACKNOWLEDGEMENTS.....	iii
INTRODUCTION .....	1
MATERIALS and METHODS.....	10
<i>Reagents and Materials</i> .....	10
<i>Solutions</i> .....	12
<i>Preparing nitrocellulose strips spotted with anti-CRP</i> .....	12
<i>Preparing nitrocellulose strips striped with anti-CRP and anti-rbIFNT</i> .....	13
<i>Performing half-strip assays with anti-CRP strips</i> .....	14
<i>Performing half-strip assays with striped anti-rbIFNT</i> .....	15
<i>Capillary-driven immunoassay (CaDI) tests</i> .....	15
<i>Setting up lateral-flow assays</i> .....	17
<i>Performing tests with lateral-flow assays</i> .....	18
RESULTS.....	19
<i>Half-strip assays with spotted anti-CRP strips</i> .....	19
<i>Half-strip assays with striped-anti-CRP strips</i> .....	20
<i>Half-strip assays with striped anti-rbIFNT strips</i> .....	31
<i>Capillary-driven immunoassays (CaDI)</i> .....	33
<i>Lateral flow assay format</i> .....	37
DISCUSSION.....	42
CONCLUSION.....	46
REFERENCES .....	49
APPENDICES .....	56

## INTRODUCTION

The bovine estrous cycle consists of the luteal and follicular phases, and lasts from 18-24 days. In the follicular phase, the progesterone level is decreased and levels of gonadotropin-releasing hormones (GnRH) and estrogen are increased. During this phase, a dominant ovarian follicle, which contains an egg (ovum) and granulosa cells which release estrogen, is formed. During the entire estrous cycle, an average of three or four groups of ovarian follicles form in waves, but these regress early in the cycle except for the dominant ovarian follicle later in the cycle, which grows larger under low progesterone conditions. This phase includes heat and ovulation, where follicle stimulating hormone (FSH) and luteinizing hormone (LH) are released by the pituitary gland in the brain in response to GnRH and sent to the ovary via blood. FSH is responsible for forming the dominant ovarian follicle, while LH causes the follicle to rupture about 24-32 hours later, causing the release of an egg and ovulation.

In the luteal phase, a corpus luteum (CL) is formed from the remnants of the ruptured ovarian follicle and levels of oxytocin and progesterone are increased, while levels of gonadotropin-releasing hormones (GnRH) decrease (Niswender et al., 2000). A CL is a transient endocrine gland which undergoes dynamic changes, both molecular and structural, and contains luteal endothelial cells (LECs) which produce progesterone (Meidan & Basavaraja, 2022). The CL grows over the next 10 days, with peak progesterone production at around day 12 of the estrous cycle. In the case of no egg fertilization or early embryo failure, luteolysis occurs and prostaglandin F2-alpha is released, causing the CL to be destroyed. Due to the drop in progesterone, the dominant ovarian follicle forms and restarts the cycle (Medicine, 2021). The luteal phase begins between about days 1 and 4-5 of the estrous cycle, while the follicular phase

begins between about days 18 and 20 of the estrous cycle (**Figure 1**) (*The GENEX Blog: Dairy Synchronization: A Learning Experience - Part 1*, n.d.).

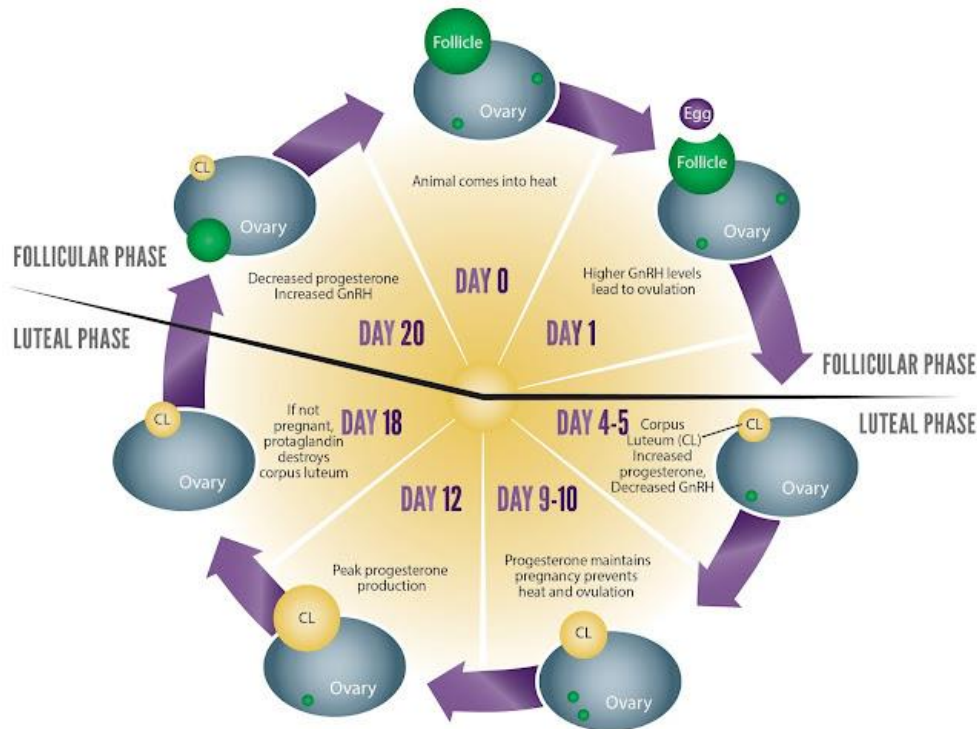


**Figure 1.** The bovine estrous cycle consists of the follicular and luteal phases, with fluctuations of progesterone and gonadotropin-releasing hormones (GnRH) as the corpus luteum forms and is destroyed.

Interferon-tau (IFNT) is the main signal in the maternal recognition of pregnancy, which involves signaling from the conceptus to the maternal system and a prolonged lifespan of the CL. Initially called a trophoblastic protein (TP-1), it was later discovered that it was a type 1 interferon, or IFNT. The molecule has a molecular weight of 19-24 kDa and is made up of 172 amino acids. In pregnant cows, evidence of IFNT secretion by trophoblast cells of the conceptus, or elongating embryo, has been observed during days 7-28 of the estrous cycle, but peaks near days 18-20, which coincides with the same time period that prostaglandin F2-alpha would have been released in a non-pregnancy scenario. IFNT has antiluteolytic effects and acts by suppressing endometrial receptors for oxytocin or estrogen, which stops the release of progesterone F2-alpha (Bazer et al., 2018; Meidan & Basavaraja, 2022).

In the dairy industry, maintaining non-pregnant (open) cows is expensive, as these cows are not lactating. Artificial insemination (AI) is used to inseminate dairy cows, but is often required to be done multiple times. Up to 80% of embryonic losses occur during the first 3 weeks after insemination, especially between days 7 and 16 post-AI (Albaaj et al., 2022; Spencer et al., 2016). Due to this, pregnancy diagnosis is part of a reproductive management program, with incentive to provide earlier pregnancy diagnosis. The current gold standard for confirming pregnancy in cows is a rectally-guided ultrasound on day 32 after insemination, and trans-rectal palpation between days 32 and 35 can also be used. However, trans-rectal palpation is invasive and can cause loss of pregnancy, and ultrasound does not provide the desired early diagnosis (Abbitt et al., 1978; Hansen et al., 2017; Vaillancourt et al., 1979). Up to \$47 a week could be returned as profit to a dairy farmer by improving early pregnancy diagnosis between inseminations, as resynchronization methods can be used to more rapidly return a cow to breeding (Cabrera, 2014). Such methods include treatment with prostaglandin-F2 alpha to shorten the luteal phase and lyse the CL, which can result in a return to breeding within 3 days of an open diagnosis (*Prostaglandin Based Estrus Synchronization in Postpartum Dairy Cows: An Update*, n.d.).

Another biomarker associated with pregnancy in cows is pregnancy specific protein B (PSPB). PSPB, a pregnancy-associated glycoprotein (PAG), has been observed in the trophoblast, or the cells surrounding the blastocyst that assist in implantation and placenta formation, as early as day 21 of pregnancy, and can be detected in blood at around day 32 of pregnancy (Humblot et al., 1988; Kawaguchi et al., 2016; Sasser et al., 1986, 1989; Szenci et al., 1998). However, it has a long half-life and can cause issues with pregnancy diagnosis within 70 days postpartum, reducing the effectiveness of testing on non-virgin heifers (Kiracofe et al.,

1993). PSPB is already used in a commercially available product called BioPRYN. It is an ELISA test which requires a blood sample, and is useful in pregnancy detection between days 25 and 28 post breeding for dairy heifers and adult dairy cows, respectively (“BioPRYN for Dairy Cattle - the Blood Pregnancy Test,” n.d.). This format also lacks the ease of access provided by point-of-care tests like lateral flow assays (LFAs). The Alertys OnFarm Pregnancy Test is another product on the market that targets PAGs. It is also a blood test that can be used 28 days post breeding and 70 days post calving. Unlike BioPRYN, the test from Alertys uses an LFA format, with results readable within 5-20 minutes (*Alertys OnFarm Ruminant Pregnancy Test - IDEXX US*, n.d.). However, this test still does not provide the early diagnosis that could be achieved with a biomarker like IFNT.

Lateral flow assays (LFAs), also known as rapid, immunochromatographic test strips or lateral flow immunoassays (LFIAs), were first developed from the latex agglutination assay. In this test, a saliva, urine, blood, or cerebrospinal fluid sample was sent to a lab and mixed with latex beads coated in a specific antigen or antibody. A positive result would be indicated by clumping together of the latex beads, or agglutination (*Latex Agglutination Test*, n.d.). One of the first applications of this was back in 1956 for serological diagnosis of rheumatoid arthritis (Plotz & Singer, 1956). The human pregnancy test detecting human chorionic gonadotropin (hCG) in the 1980’s was a major milestone in LFA development, but it is important to note that this was not possible without development of other technologies, including fluid dispensing/processing equipment and nitrocellulose membrane manufacturing.

A lateral flow assay consists of several key components: a sample pad, a conjugate pad, a nitrocellulose membrane containing a test and control line, and a waste pad. All the materials are mounted on a backing card that uses a pressure-sensitive adhesive, and different materials overlap to provide continuous, linear flow through the device (**Figure 2**). Sample is added to the sample pad, which can be pre-treated depending on the sample medium (Mahmoudi et al., 2020). The sample then flows towards the conjugate pad, where it interacts with an immobilized conjugate which consists of either antibody or antigen bound to a particle that will produce a colored signal when the particles aggregate at the test line. This complex then flows through the nitrocellulose membrane, or the reaction matrix. In this region, antibody or antigen has been immobilized to a porous membrane in different bands. The waste pad at the end is a passive driving force that wicks liquid sample through the device and into the absorbent pad.

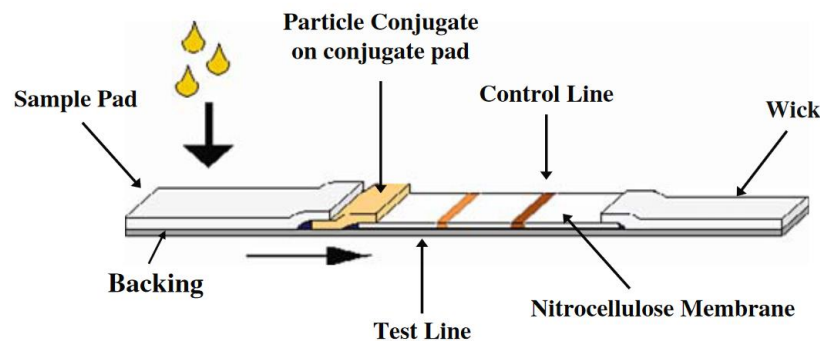


**Figure 2.** Configuration of a lateral flow assay (LFA)

In a direct format, which is better for high molecular weight analytes that can bind two antibodies at the same time, the test line serves to capture the complex consisting of analyte-labeled secondary antibody, while the control line serves to capture unbound labeled secondary antibody. For a positive result, both lines would show a signal, while a negative result would only show signal in the control line. In a competitive format, which is best for low molecular weight analytes that cannot bind two antibodies at the same time, signal in the control line

indicates a positive result, while signal in both the test and control lines is a negative result. This format is often achieved by immobilizing capture antibody already bound to antigen at the test line (O'Farrell, 2008). Tests can also be multiplexed to detect multiple analytes, which is done by including multiple test lines.

LFAs are point-of-care (POC) tests and popular due to their ease-of-use, low cost, and availability for rapid testing versus plate-based formats like enzyme-linked immunosorbent assay (ELISA), where a skilled lab technician or expensive robot is required and results can take hours to obtain (Calabria et al., 2021; Sajid et al., 2015). In a sandwich ELISA, antibodies are immobilized onto a solid plastic support. If antigen is present, it is captured and interacts with a secondary antibody that is bound to an enzyme, which converts substrate to yield a measurable visible signal. The concentration of antigen can be calibrated to the signal intensity, which is proportional to concentration.

Horseradish peroxidase (HRP) is the most common enzyme used in ELISA, as it has multiple available substrates and demonstrates strong catalytic activity. 3,3',5,5'-Tetramethylbenzidine (TMB) converts to an oxidized form, diamine, when TMB is reacted with hydrogen peroxide and catalyzed by HRP (**Figure 3**). A blue color is first formed, followed by a yellow color after the addition of stopping solution, which consists of phosphoric or sulfuric acid. Quantitatively, the absorbance can be measured at 450 nm after the addition of stopping solution. Other chromogenic, or color-producing, substrates for HRP include 2,2'-Azinobis (3-

Ethylbenzothiazoline-6-Sulfonic Acid) Diammonium Salt (ABTS), o-phenylenediamine dihydrochloride (OPD), and diaminobenzidine (DAB) (Tabatabaei & Ahmed, 2022).

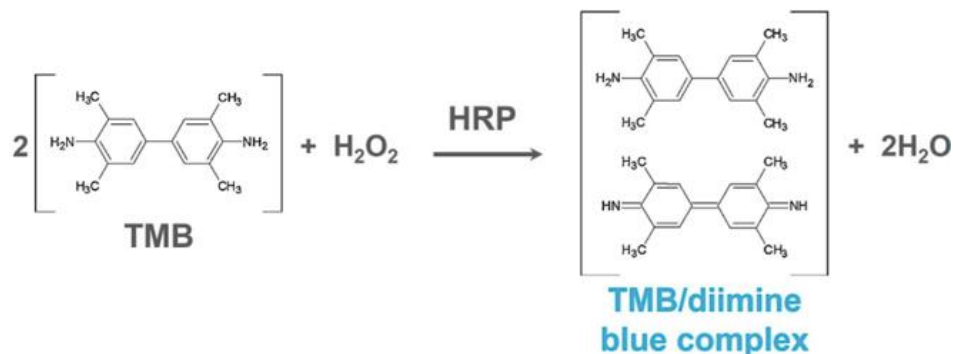


**Figure 3.** TMB is oxidized in a reaction with hydrogen peroxide that is catalyzed by HRP.

The set-up of a sandwich ELISA can be adapted for a lateral flow assay to amplify signal from 5 to 100-fold (Calabria et al., 2021). A lateral flow enzyme immunoassay (LFEIA) that detects progesterone in cow's milk was developed using HRP and TMB, with a detection limit of 0.8 ng/mL (Samsonova et al., 2015). In another test designed to detect human IgG, gold nanoparticles were modified with enzymes to provide an enhanced signal, with the option of measuring with a strip reader before and after the addition of substrate (Parolo et al., 2013).

Besides enzymatic reactions, signal at the test line can be conferred by gold nanoparticles, magnetic nanoparticles, colloidal carbon, and more. Gold nanoparticles are popular due to their production of a direct optical signal which is visible to the naked eye and requires no extra steps to generate. They can also be easily functionalized with biomolecules due to their high affinity. Magnetic nanoparticles can produce a signal that is more stable and sensitive than an optical signal but is also colored if optical detection is desired. Colloidal carbon can produce sensitivity comparable to ELISA due to the black color and variety of functionalities, but also has issues with non-specific adsorption of biomolecules (Sajid et al., 2015). Gold nanoparticles were used to detect Parathyroid hormone-like hormone (PTHrP) and

penicillin-binding protein 2a (PB2a) in developed lateral flow assays (Amini et al., 2020; Chamorro-Garcia et al., 2016). Detection of Ara h 1, a major peanut allergen, was provided by a test utilizing magnetic nanoparticles, with 97.6% agreement of results with an ELISA (Yin et al., 2022). Antibodies against *Mycoplasma bovis* were detected in a test utilizing colloidal carbon, or carbon nanoparticles (Shi et al., 2020).

Microfluidic devices are starting to become more common in the point-of-care field. They are often preferred due to reduced consumption of reagents, low sample volume requirements, and the ability to automate a test based on its design. They are made up of different materials, including polydimethylsiloxane (PDMS), glass and silicon, and paper-based materials. Paper-based devices are low-cost and ideal in environments with poor resources, but do suffer from temperature and humidity sensitivity (Nsamela, 2020; Yang et al., 2022).

Investigators at Colorado State University have developed a capillary-driven immunoassay (CaDI) that utilizes an enzymatic reaction comparable to a sandwich ELISA. The device is made of stacked layers of hydrophilic polyester transparency and double-sided adhesive films, and reagents are released using pre-treated glass fiber pads. Upon addition of 100  $\mu$ L of sample, the reagents are sequentially delivered to a nitrocellulose membrane that is modified with capture antibody or antigen. The test utilizes a reaction where TMB is oxidized during the enzymatic degradation of hydrogen peroxide by horseradish peroxidase (HRP) (Carrell et al., 2023; Clark et al., 2022; Samper et al., 2021).

The focus of this thesis is to develop a point-of-care (POC) test using IFNT as the biomarker for an early pregnancy test in dairy cows. While detectable by formats such as ELISA, a cow-side test for IFNT would be an improvement over current technology (*Bovine Interferon Tau (IFN $\tau$ ) ELISA Kit, Cat#EKU09093*, n.d.). Methods with nitrocellulose were first optimized

using C-reactive protein (CRP) and gold nanoparticles as the detection particle. Subsequently, a capillary-driven immunoassay (CaDI) and hybrid lateral flow assay (LFA) were explored in the development of the final test, which utilizes a lateral flow assay format and the enzyme HRP and the substrate TMB to amplify signal at the test line.

## MATERIALS and METHODS

The aim of this research was to create a cow-side test using interferon-tau (IFNT) as the biomarker. Several different tests were explored, including a capillary-driven immunoassay (CaDI) and a sandwich lateral flow assay (LFA) utilizing an enzymatic reaction with TMB as the substrate and HRP as the enzyme. Before these tests could be optimized, development of a half-strip assay was conducted with C-reactive protein (CRP) and a secondary antibody conjugated with gold nanoparticles (GNP). This was then translated to a half-strip assay using recombinant IFNT (rbIFNT) and a secondary antibody conjugated with horseradish peroxidase (HRP) for signal amplification. Several methodological limitations were discovered, including a required wait time after capture antibody was striped onto nitrocellulose and precise technique required when loading sample into the wells of the BioSpot to avoid bubble formation and loss of antibody solution.

### *Reagents and Materials*

Recombinant IFNT (rbIFNT), rbIFNT polyclonal rabbit antibody, biotinylated rbIFNT polyclonal rabbit antibody, and rbIFNT polyclonal goat antibody were obtained from Colorado State University. Horseradish peroxidase conjugated streptavidin (21126) was obtained from Thermo Fisher Scientific. BioFX<sup>®</sup> TMB One Component HRP Membrane Substrate was obtained from Surmodics. HRP Conjugation Kit – Lightning Link<sup>®</sup> (ab102890) was purchased from Abcam.

C-reactive protein (CRP) (30-AC05S) was purchased from Fitzgerald. CRP polyclonal goat antibody (PAB7943) and biotinylated CRP monoclonal mouse antibody (MAB5101) were purchased from Abnova. 20 and 30 nm Streptavidin – Gold Conjugates, which were both

passively and covalently conjugated, were obtained from Cytodiagnostics. Passively conjugated gold conjugates rely on passive adsorption, or electrostatic and hydrophobic forces interacting between the gold nanoparticle surface layer and streptavidin. Covalent conjugation uses a chemical linker to permanently immobilize streptavidin onto gold nanoparticles and minimize phenomena such as steric hindrance (*Covalent Conjugation of Proteins to Carboxylated Gold Nanoparticles*, n.d.).

Casein, bovine serum albumin (BSA), D-mannitol, and boric acid were purchased from Thermo Fisher Scientific. Phosphate buffer saline (PBS) tablets, sodium hydroxide, D-(+)-trehalose dihydrate, thimerosal, Tween-20, sucrose, Tris(hydroxymethyl)-aminomethane (Tris), and sodium tetraborate were purchased from Sigma-Aldrich. Glycerol was purchased from Mallinckrodt, and Tris HCl was obtained from J.T. Baker. Sodium chloride was purchased from Oakwood Chemical.

Whatman FF80HP nitrocellulose was purchased from Cytiva and Vivid™ nitrocellulose (VIV902550R) was purchased from Pall. Glass fiber conjugate pad (GFCP000800) was obtained from Sigma Aldrich and backing cards (MIBA-010) were purchased from DCN Diagnostics. Whatman Grade 1 Chr Chromotography paper was purchased from Cytiva and used as the material for the waste pad. 467 double-sided adhesives (DSA) and polyethylene terephthalate (PET) sheets (9984) were obtained from 3M.

A CO<sub>2</sub> laser cutter (Zing 10000, Epilog Laser) was used to etch and cut nitrocellulose into strips, cut microfluidic channels for the capillary-driven immunoassay, and cut backing cards to size. A BioFluidix BioSpot® BT600 was used to stripe antibody onto nitrocellulose. ImageJ, an image-based processing program, was used to provide quantitative results for test strips by measuring mean gray value (*Analyze Menu*, n.d.).

## *Solutions*

Solutions were prepared using DI water from a Milli-Q system obtained from Millipore Sigma. 10 mM phosphate buffer solution (PBS) with 140 mM sodium chloride and 2.7 mM potassium chloride (pH 7.4) was prepared by dissolving a tablet in 500 mL of DI water. PBS with 1% BSA was prepared by dissolving 1 g of BSA in 100 mL of 10 mM PBS. Pre-treatment solution with 0.1% thimerosal, 0.5% Tween-20, and 3% sucrose was prepared by dissolving 0.1 g of thimerosal, 450  $\mu$ L of Tween-20, and 3 g of sucrose in 10 mM PBS. Tris buffer was made by dissolving 1.515 g of Tris and 4.385 g of sodium chloride in 500 mL DI water. The sugar-salt solution used to coat over capture antibody in an alternative striping condition was made by dissolving 2.922 g of sodium chloride, 6 g of D-mannitol, 6.63 g of D-(+)-trehalose dihydrate, 10 g of glycerol, 0.254 g of Tris HCl, and 0.0472 g of Tris base in 100 mL of DI water. Previously, a bulk solution of 6% aged casein in 50 mM borate buffer was prepared by dissolving 6 g of casein in 80 mL of 50 mM sodium hydroxide overnight, adding 0.26 g boric acid and 0.45 g sodium tetraborate, and adjusting the pH to 8.5. The solution volume was adjusted to 100 mL with DI water followed by heating for 7 days at 37 °C. The resulting solution, aged casein, was aliquoted and stored at -20 °C for future use and dilution in 50 mM borate buffer (Clark et al., 2022; Samper et al., 2021).

## *Preparing nitrocellulose strips spotted with anti-CRP*

A CRP polyclonal goat antibody (anti-CRP) was applied to FF80HP nitrocellulose using a pipette. The 1 mg/mL antibody solution had 0.044 M D-(+)-trehalose dihydrate and 4.44% glycerol in phosphate-buffered saline (PBS). Before application of antibody solution, nitrocellulose was etched and cut into strips (15 mm  $\times$  4 mm) using a CO<sub>2</sub> laser cutter. 0.25  $\mu$ L of antibody solution was applied at a time, with a 7-min drying period in a drying oven at 37°C

after the first 3 applications, followed by a 45-min drying period at the same temperature after the fourth addition. Blocking was performed by filling a petri dish with StabilGuard™ and dipping the ends of the strips, with solution wicking upwards towards the waste pad section. Strips were then dried for 1 h in a drying oven at 37°C before final storage with a desiccator pouch in a petri dish in a fridge at 4°C. The petri dish was wrapped in parafilm to preserve the dry environment.

For the experiment utilizing the second blocking protocol, strips were dried for 10 min at 37°C after the fourth addition, followed by overnight storage in a desiccator. Strips were then blocked and dried for 5 h at 37°C before final storage, which was identical to the above method.

#### *Preparing nitrocellulose strips striped with anti-CRP and anti-rbIFNT*

A CRP polyclonal goat antibody (anti-CRP) or an rbIFNT polyclonal goat antibody (anti-rbIFNT) was applied to nitrocellulose by striping with a BioSpot, with FF80HP membrane for the anti-CRP and Vivid-90 membrane for anti-rbIFNT. Before antibody application, the nitrocellulose was etched with a laser cutter. 20 µL of 1 mg/mL antibody solution with 0.044 M D-(+)-trehalose dihydrate and 4.44% glycerol in phosphate-buffered saline (PBS) was loaded into the well for striping, 5 mm from the start of the waste pad section.

Two protocols were tested for blocking with Stabilguard™. In the first, the nitrocellulose was dried for 45 min after striping, followed by blocking. The nitrocellulose was then dried for 1 h in a drying oven at 37°C before being cut into strips using a laser cutter. Final storage was with a desiccator pouch in a petri dish at room temperature (RT). The petri dish was wrapped in parafilm and covered in aluminum foil to preserve the dry environment and avoid exposure to light. In the second protocol, the nitrocellulose was stored overnight in a desiccator after striping.

Blocking was performed, and the nitrocellulose was dried for 5 h in a drying oven at 37°C. The nitrocellulose was then cut into strips and stored as in protocol 1.

To prepare double-striped strips, another layer (20  $\mu$ L) of antibody solution was applied by filling the first well with extra solution. The second layer was applied 10 min after the first to let drying occur. The second blocking protocol was then followed. For strips utilizing the alternative striping method that includes coating a sugar-salt solution over the capture antibody, the protocol for double-striped strips was used, with sugar-salt solution in place of the second antibody layer and solution being added into the second well in the BioSpot.

#### *Performing half-strip assays with anti-CRP strips*

Previously, a layer of PET film was sandwiched with layers of double-sided adhesive to create a PET layer with sticky outer surfaces. Rectangular sections (2 cm wide) were cut, and the sticky PET layer was adhered to PET film by removing the outer paper layers. Nitrocellulose strips spotted or striped with anti-CRP were attached at the waste pad section, with the rest of the strip hanging below the adhesive. Strips were raised by 45° to promote flow through the porous membrane. The waste pad section was covered with a waste pad, and reagents were applied 1  $\mu$ L at a time to the other end of the nitrocellulose with a pipette. CRP or dilution buffer (10 mM PBS) was added first, followed by biotinylated CRP monoclonal mouse antibody and streptavidin-conjugated GNP (0.5 mg/mL), each of which was added in final volumes of 5  $\mu$ L. Washing with 10 mM PBS was done between the addition of each reagent and after the final application, with increasing volumes to wash away unbound reagents (5  $\mu$ L, then 10  $\mu$ L, then 15  $\mu$ L). Strips were then detached from the double-sided adhesive and photographed in a light box.

### *Performing half-strip assays with striped anti-rbIFNT*

Half-strip assays with striped anti-rbIFNT were conducted in a similar manner but with different reagents. rbIFNT or dilution buffer (10 mM PBS) was added first, followed by biotinylated rbIFNT polyclonal rabbit antibody, streptavidin conjugated HRP, and TMB. A final wash step of 10  $\mu$ L was added to wash away insoluble oxidized TMB product that was non-specifically bound to the nitrocellulose.

### *Capillary-driven immunoassay (CaDI) tests*

Three layers of PET film (100  $\mu$ m thick) were sandwiched with two layers of double-sided adhesive (50  $\mu$ m thick) to form a device with 3D microfluidic channels. A CO<sub>2</sub> laser cutter was used to cut the device layers from a design in CorelDRAW, as observed in **Figure 4**. TMB and conjugate pads were placed in the device channels before sealing the device with the top layer of PET film, which has square cutouts directly over the pads to avoid creating a vacuum within the device. Pressure was applied to the cover to restrict liquid flow outside of the microfluidic channels. The TMB pad was placed where the blue pad is located in **Figure 4**, while the conjugate pad was placed where the yellow pad is located. A nitrocellulose strip striped with anti-rbIFNT was inserted at the outlet of the microfluidic network, and the device was pressed onto parallel sticky PET layers, which bound to the microfluidic device and the waste pad section of the nitrocellulose strip. A waste pad was added at the end of the nitrocellulose strip to draw liquid through the strip.

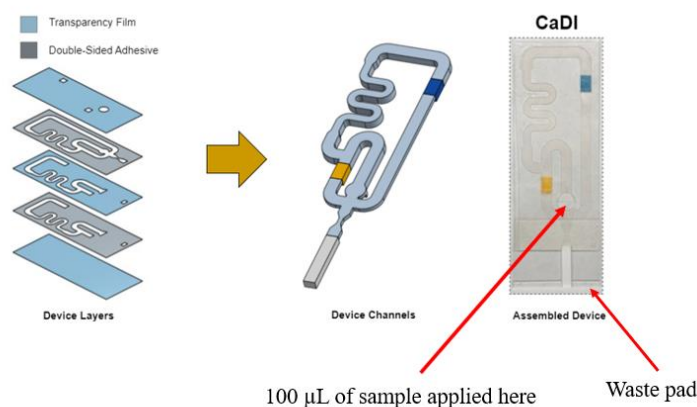


**Figure 4.** Layers of the CaDI device consist of hydrophilic PET film and double-sided adhesive. When fully constructed, 3D microfluidic channels are formed with slots for the TMB and conjugate pads, indicated by the blue and yellow squares, respectively.

TMB and conjugate pads were prepared using pretreated glass fiber pads. Glass fiber pads were pre-treated by soaking in a solution of 0.1% thiomersal, 0.5% Tween 20, and 3% sucrose in 10 mM PBS for 15 min at room temperature (RT) before drying overnight at 37°C in a drying oven. Pads were then cut to size (5 mm × 3 mm) and stored at room temperature (RT) in a petri dish before use. For TMB pads, 7.5 µL of TMB was applied 3 times using a pipette, with 7 min of drying at 37°C between the first and second applications. After the final addition, the pads were dried for 2 h at the same temperature. For conjugate pads, blocking was first done, followed by application of the HRP-antibody conjugate. Conjugate pads were blocked by adding 7.5 µL of 0.57% aged casein in 50 mM borate buffer twice, drying at 37°C for 7 min after the first application and for 30 min after the second application. After blocking, 5 µL of polyclonal rabbit anti-rbIFNT conjugated with horseradish peroxidase (HRP) was added, followed by drying at 37°C for 30 min. Conjugates developed using a biotin-streptavidin bond were tested with CaDI. Biotinylated polyclonal rabbit anti-rbIFNT was mixed with streptavidin-conjugated HRP and reacted at room temperature (RT) for 45 min in a 1:3 molar ratio (and 1:2 volume ratio). This was diluted in 10 mM PBS with 1% BSA before application to the conjugate pad.

For dye experiments, which were conducted to better observe flow of reagents within the device, 5  $\mu\text{L}$  of blue or yellow Great Value food dye (diluted 80 $\times$  in DI water) was applied to the pads after conjugate or TMB was added and dried at 37°C for 1 h. Blue dye was added to the TMB pads and yellow dye was added to the conjugate pads. Dye-only experiments were also conducted in order to limit reagent consumption during improvement of the sample application methodology. For these experiments, non-pretreated glass fiber pads were prepared using only dye in a similar manner.

100  $\mu\text{L}$  of sample or dilution buffer (10 mM PBS) was added to the circular inlet using a pipette. The test was observed for 15 min while reagents were delivered to the test line, and the nitrocellulose strips were removed and imaged in a light box after this time period (Clark et al., 2022; Samper et al., 2021).

#### *Setting up lateral-flow assays*

The set-up of each lateral flow assay (LFA) included a sample pad, conjugate pad, nitrocellulose strip, waste pad, and backing card (48 mm  $\times$  4 mm). Glass fiber pads were pre-treated by soaking in a solution of 0.1% thiomersal, 0.5% Tween 20, and 3% sucrose in 10 mM PBS for 15 min at room temperature (RT) before drying overnight at 37° C in a drying oven. Pads were then cut, with dimensions of 18 mm x 8 mm for sample pads and 9 mm x 8 mm for conjugate pads. Pre-treated pads were stored in a petri dish at room temperature (RT) before use.

Conjugate pads were blocked by adding 25  $\mu\text{L}$  of 0.57% aged casein in 50 mM borate buffer twice, drying at 37°C for 30 min after the first application and for 1.5 h after the second application. After blocking, 15  $\mu\text{L}$  of polyclonal rabbit anti-rbIFNT conjugated with horseradish peroxidase (HRP) was added, followed by drying at 37°C for 1 h.

Conjugates developed using a biotin-streptavidin bond and a lightning kit were both tested during LFA development. For the biotin-streptavidin bonded conjugate, biotinylated polyclonal rabbit anti-rbIFNT was mixed with streptavidin-conjugated HRP and reacted at room temperature (RT) for 45 min in a 1:3 molar ratio (concentrations adjusted for a 1:2 volumetric ratio). Lightning kit conjugates were prepared as instructed, with a 3 h reaction period before quenching solution was added, and diluted in 10 mM PBS with 1% BSA. Sample and conjugate pads were stored with a dessicator pouch in a petri dish at 4°C. The petri dishes were wrapped in parafilm and aluminum foil.

#### *Performing tests with lateral-flow assays*

100  $\mu$ L of rbIFNT or dilution buffer (10 mM PBS or Tris) was added to the sample pad, and after 15 min, 100  $\mu$ L of buffer was added to remove unbound molecules. After 15 min, 3  $\mu$ L of TMB was added directly to the test line using a pipette. The reaction proceeded for 3 min before 100  $\mu$ L of wash buffer was added to the sample pad to remove non-specific insoluble oxidized TMB product. Strips were imaged in the light box after removing everything from the backing but the nitrocellulose strip, which was not removed to avoid damage to the strip.

## RESULTS

### *Half-strip assays with spotted anti-CRP strips*

CRP was initially used as the target protein prior to turning to rbIFNT in order to develop and improve the methodology with nitrocellulose before using more expensive reagents. Half-strip assays were first used to reduce complexity of the design – by eliminating the sample and conjugate pads, fewer variables were under consideration and the focus could be shifted to binding activity at the test line and how changes in protocol affected this. The main variable under consideration in the spotted anti-CRP half-strip assays was the size of the gold nanoparticles in the streptavidin-gold conjugate.

To investigate this variable, concentrations of CRP and biotinylated secondary antibody of 1000  $\mu\text{g/mL}$  and 100  $\mu\text{g/mL}$ , respectively, were tested with both sizes of gold nanoparticles and passively-conjugated streptavidin-gold conjugates. The results in **Figure 5** show that 20 nm provided increased signal over 30 nm, with purple dots representing binding of the antigen and secondary antibody to the test spot. Further testing with 20 nm gold nanoparticles and increased concentrations of CRP and biotinylated secondary antibody (2550  $\mu\text{g/mL}$  and 1000  $\mu\text{g/mL}$ ) demonstrated a strong signal that was interpreted as strong enough to move on to the striping phase, as shown by **Figure 6**. However, there was evidence of background signal, particularly with the second experiment. At this point, it was decided to move forward with 30 nm gold nanoparticles to reduce the risk of background signal.

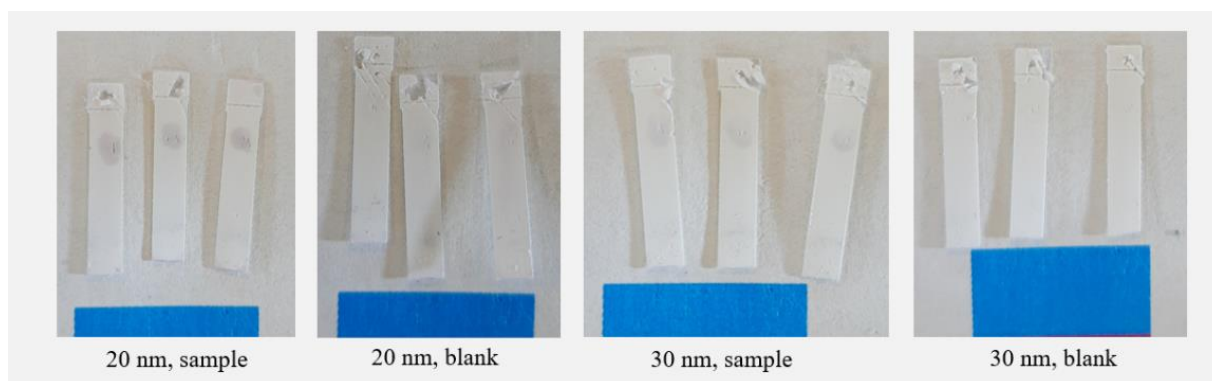


**Figure 5.** Results of half-strip assays tested with spotted anti-CRP strips and different sizes of gold nanoparticles (GNP). CRP and biotinylated secondary antibody concentrations of 1000  $\mu\text{g/mL}$  and 100  $\mu\text{g/mL}$  were used. 20 nm GNP resulted in stronger signal in sample strips, but also stronger background signal in blank strips.

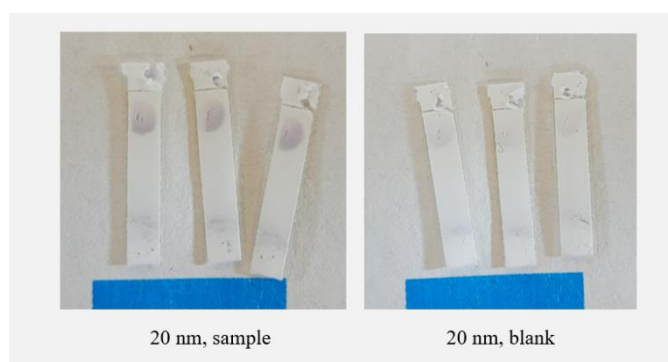


**Figure 6.** Results of half-strip assays tested with spotted anti-CRP strips and 20 nm GNP. CRP and biotinylated secondary antibody concentrations of 2550  $\mu\text{g/mL}$  and 1000  $\mu\text{g/mL}$  were used. The signal in sample strips was strong, but some background signal was also present in the blank strips.

### *Half-strip assays with striped-anti-CRP strips*

One of the first variables tested with striped anti-CRP strips was the conjugation method of the streptavidin-gold conjugate: passive vs. covalent. Results of this experiment, which used CRP and biotinylated secondary antibody concentrations of 1000  $\mu\text{g/mL}$  and 100  $\mu\text{g/mL}$ ,

respectively, and the first protocol for blocking, showed that covalent conjugation provided a much stronger signal when sample was tested (**Figure 7**).



**Figure 7.** Results of half-strip assays tested with spotted anti-CRP strips and different methods of conjugation for the gold nanoparticles conjugated with streptavidin. Strips on the left were tested with a conjugate that was covalently conjugated, while strips on the right were tested with a conjugate that was passively conjugated. CRP and biotinylated secondary antibody concentrations of 1000  $\mu\text{g}/\text{mL}$  and 100  $\mu\text{g}/\text{mL}$  were used. Covalent conjugation resulted in stronger signal than passive conjugation methods, and a red-colored signal instead of a purple-colored signal.

Further experimentation was done with the covalently conjugated streptavidin-gold conjugate, with attempts to reduce the CRP concentration. CRP concentrations of 100 and 10  $\mu\text{g}/\text{mL}$  with biotinylated secondary antibody at 10  $\mu\text{g}/\text{mL}$  showed strong results (**Figure 8**), with only slight background signal in the blank strips. The second blocking protocol was also tested with 10  $\mu\text{g}/\text{mL}$  CRP. Results of this experiment showed a similar signal in the sample strips, with no evidence of background signal in the blank strips (**Figure 9**).

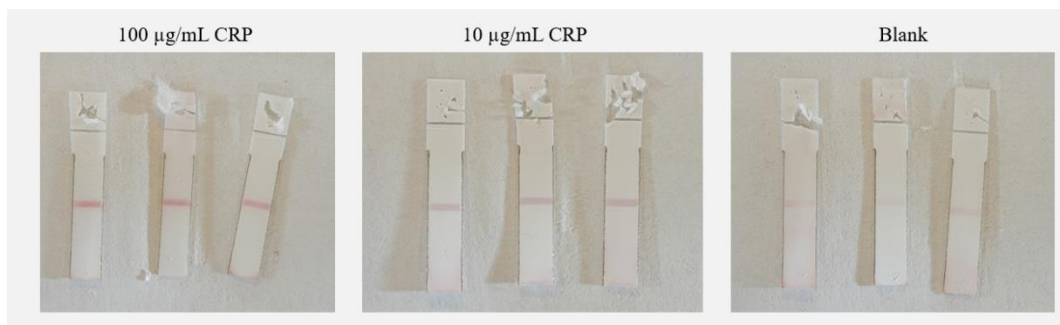


**Figure 8.** Results of half-strip assays tested with striped anti-CRP strips that were blocked with the first protocol. A biotinylated secondary antibody concentration of 10  $\mu\text{g}/\text{mL}$  was used. The signal in both sets of sample strips was strong, with slight background signal in the blank strips.

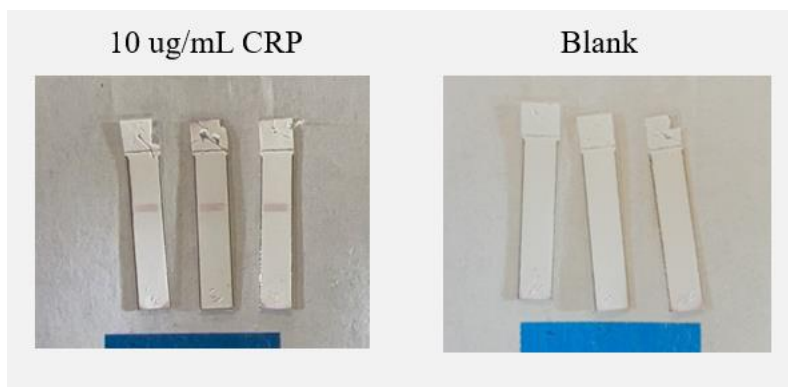


**Figure 9.** Results of half-strip assays tested with striped anti-CRP strips that were blocked with the second protocol. A biotinylated secondary antibody concentration of 10  $\mu\text{g}/\text{mL}$  was used. The results were like tests with the first blocking protocol, but with no background signal in the blank strips.

Future experiments at lower concentrations of CRP failed to produce a signal in sample or blank strips, so higher concentrations of CRP (100  $\mu\text{g}/\text{mL}$ ) were tested for reproducibility. Once again, no signal in sample or blank strips was observed. These experiments shared one common condition: the strips were produced (striped and blocked) at least 6 days ago. This led to a major realization of one of the limitations of this research: strips that were striped with antibody stopped working six days after production. In response to this realization, several strategies were taken, including re-evaluating spotted CRP strips made several months ago, continuing to evaluate blocking protocols 1 and 2, and testing strips weeks after their production in a process called aging.

Spotted strips made with the first and second blocking protocols 3 months previously were tested with high concentrations of CRP and biotinylated antibody (1000  $\mu\text{g}/\text{mL}$  and 100  $\mu\text{g}/\text{mL}$ , respectively). While no signal resulted with the first protocol, the signal with the second

protocol was strong, which indicated some long-term stability with this protocol for spotted strips (**Figure 10**).



**Figure 10.** Results of half-strip assays tested with spotted anti-CRP strips (aged 3 months) that were blocked with the second protocol. CRP and biotinylated secondary antibody concentrations of 1000  $\mu\text{g}/\text{mL}$  and 100  $\mu\text{g}/\text{mL}$  were used. Blank strips are not pictured, but had no background signal. The first blocking protocol was also tested with spotted strips aged 3 months, but no signal was observed.

At this point, another unexpected observation occurred: strips appeared to process a smaller volume of liquid in the half-strip format, with up to half of test strips during each experiment (3 strips for the sample, 3 strips for the blank) forming pools of liquid at the site of application. The result of this was fewer replicates, as some strips never wicked liquid from the pool to the waste pad and others absorbed the liquid so slowly that their testing was discontinued to preserve results from other strips that appeared to function properly. This could also be the cause of the false positives observed in later experiments, as slow flow was found to be associated with increased non-specific binding.

High concentrations of CRP and biotinylated antibody (1000  $\mu\text{g}/\text{mL}$  and 100  $\mu\text{g}/\text{mL}$ , respectively) were tested with 1-day old nitrocellulose strips using a CRP source without sodium azide and both blocking protocols. Tests with the first blocking protocol resulted in intense pooling which led to no results, while tests with the second blocking protocol resulted in strong

signal in the sample strips and no background signal in the blank strips (**Figure 11**). This led to the continuation of the second blocking protocol for future experiments. Tests on days 3 and 8 after antibody stripping and blocking were also conducted with 100  $\mu\text{g/mL}$  CRP, with declining signal on day 3 and no signal by day 8 (**Figure 12**). However, it is important to note that the reduction in signal could be due to the lack of sodium azide in the CRP. Due to the declining signal intensity that was harder to detect by eye, analysis using ImageJ was employed to differentiate between sample and blank strips (**Figure 17**). This analytical method involves measuring the signal of the test line (mean T) and the background (mean B) and calculating the mean gray ratio (GR), where mean GR is equal to mean T divided by mean B.

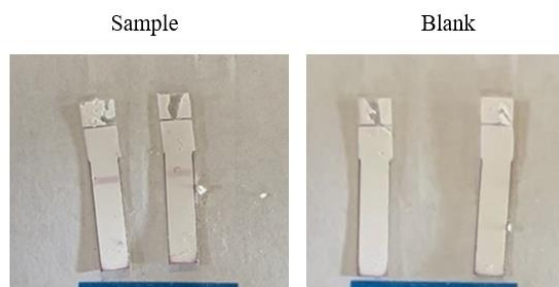


**Figure 11.** Results of half-strip assays tested with striped anti-CRP strips (aged 1 day) that were blocked with the second protocol. CRP (w/out sodium azide) and biotinylated secondary antibody concentrations of 1000  $\mu\text{g/mL}$  and 100  $\mu\text{g/mL}$  were used.

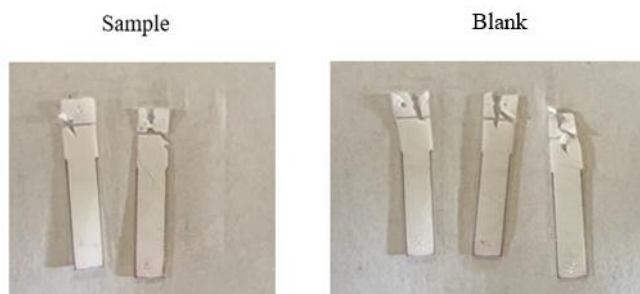


**Figure 12.** Results of half-strip assays tested with striped anti-CRP strips (aged 3 days) that were blocked with the second protocol. CRP (w/out sodium azide) and biotinylated secondary antibody concentrations of 100  $\mu\text{g/mL}$  and 10  $\mu\text{g/mL}$  were used. Signal in the test line is barely visible in both sample and blank strips.

Tests with aged strips began to produce successful results after 4 weeks, with some observance of false positive signal. Strips aged 2 weeks were tested with 100  $\mu\text{g}/\text{mL}$  CRP and 10  $\mu\text{g}/\text{mL}$  biotinylated secondary antibody, with limited success (**Figure 13**). While no signal was observed in the sample strips, background signal was observed in the blank strips, which could suggest that the capture antibody was active. However, a subsequent test with 10  $\mu\text{g}/\text{mL}$  CRP provided no signal in sample or blank strips, which challenged this notion. Strips were tested again at 4 weeks, with improved results. CRP concentrations of 241  $\mu\text{g}/\text{mL}$  and 100  $\mu\text{g}/\text{mL}$  yielded strong signal when paired with biotinylated secondary antibody concentrations that were approximately half the CRP concentration (100 and 50  $\mu\text{g}/\text{mL}$ ) (**Figure 14**). Flow issues were also much improved with the four-week-old strips, with little-to-no pooling occurring during the test. However, CRP concentrations of 10 (w/biotinylated secondary antibody 10 $\times$  lower) and 20  $\mu\text{g}/\text{mL}$  produced a barely visible signal (**Figure 15**), indicating that aged strips may not perform as well for lower concentrations of CRP. Strips aged 6.5 weeks provided potential signal at the ng/mL level, with 10 ng/mL producing signal when tested with an identical concentration of biotinylated secondary antibody (**Figure 16**). However, the issue of background signal prevailed at this low sample concentration.

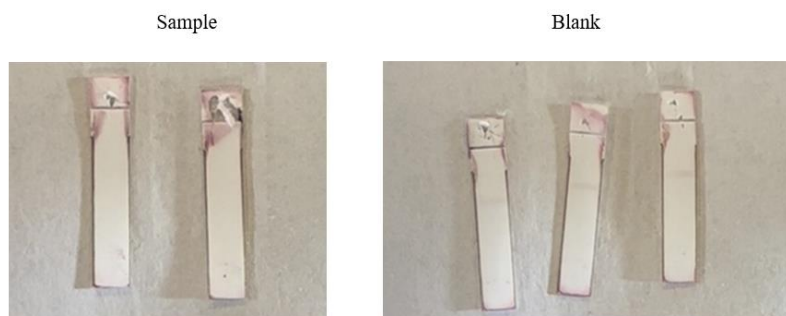


**Figure 13.** Results of half-strip assays tested with striped anti-CRP strips (aged 2 weeks) that were blocked with the second protocol. CRP and biotinylated secondary antibody concentrations of 100  $\mu\text{g}/\text{mL}$  and 10  $\mu\text{g}/\text{mL}$  were used. Signal in the test line is barely visible in both sample and blank strips, with only slightly visible background signal in the blank strips.



**Figure 14.** Results of half-strip assays tested with striped anti-CRP strips (aged 4 weeks) that were blocked with the second protocol. Biotinylated secondary antibody concentrations of 100  $\mu\text{g/mL}$  (left) and 50  $\mu\text{g/mL}$  (right) were used. Strong signal was produced in the sample strips at both CRP concentrations, and little to no background signal was present.

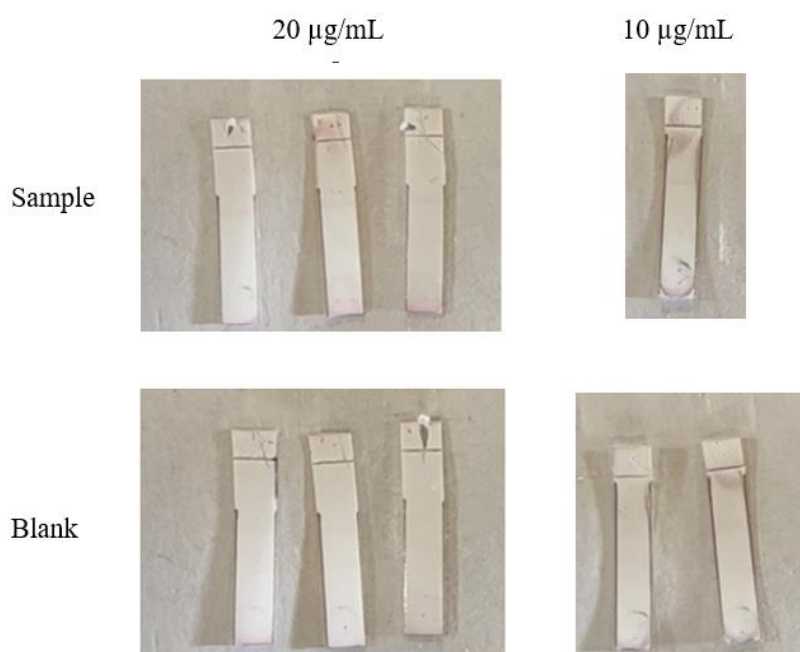


**Figure 15.** Results of half-strip assays tested with striped anti-CRP strips (aged 4 weeks) that were blocked with the second protocol. CRP concentrations of 10  $\mu\text{g/mL}$  and 20  $\mu\text{g/mL}$  were tested with biotinylated secondary antibody concentrations of 1  $\mu\text{g/mL}$  and 10  $\mu\text{g/mL}$ , respectively. Signal in the test line is barely visible in both sample and blank strips.



**Figure 16.** Results of half-strip assays tested with striped anti-CRP strips (aged 6.5 weeks) that were blocked with the second protocol. CRP and biotinylated secondary antibody concentrations of 10 ng/mL were used. Signal in the test line is barely visible in both sample and blank strips.

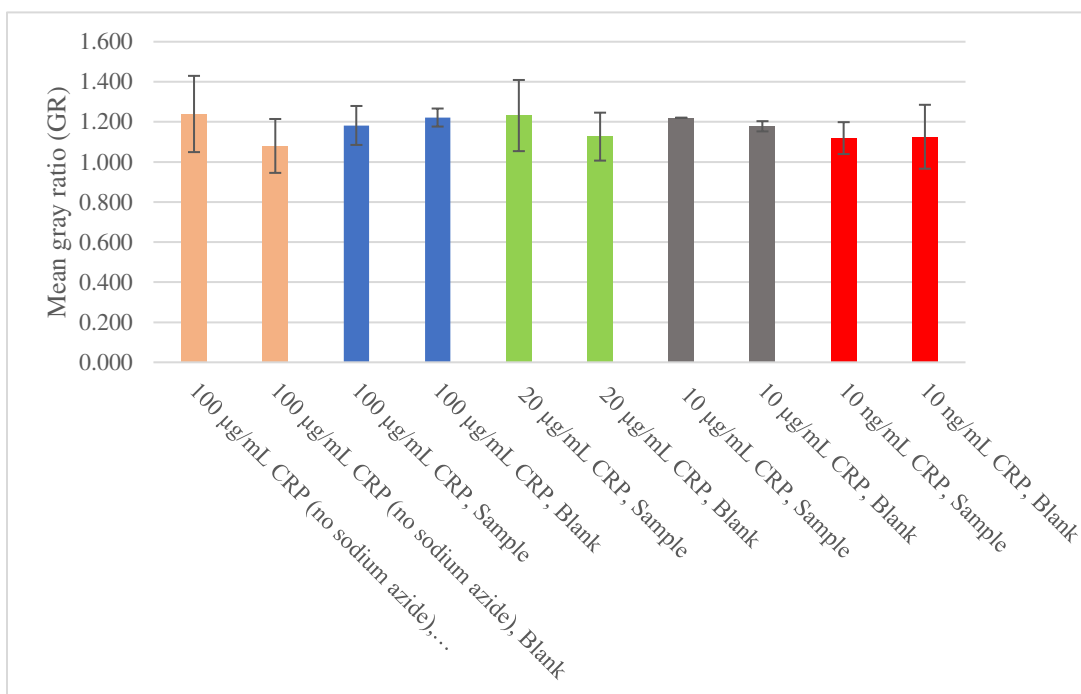


**Figure 17.** ImageJ was used to quantify results for test strips with signal that was difficult to observe with the naked eye. The mean gray ratio (GR) is a measure of the signal in the test line divided by the signal in the background. No signal is indicated by a mean GR of 1, whereas signal is indicated by a mean GR greater than 1.

Alternative striping methods at the test line were also used, such as coating a second layer of antibody solution at the same concentration (double-striped antibody) or a sugar-salt solution over the capture antibody. 50 µg/mL of CRP produced signal when paired with 10 µg/mL

biotinylated secondary antibody in 3-day old double-striped (DS) strips. However, strong background signal was also present, which could be in part due to the poor flow conditions encountered during the test, indicated by the residual traces of purple left behind on the nitrocellulose strip (**Figure 18**), with Image J results shown in **Figure 21**. 4-week-old strips with sugar-salt solution were also tested. 10 ng/mL CRP produced signal with a biotinylated secondary antibody concentration of 1 ng/mL (**Figure 19**). While the signal with these alternatives was stronger than normal strips near the same aging time period, the background signal was a drawback. To explore this, a biotinylated antibody concentration 100 times lower than the CRP concentration was tested with 1  $\mu\text{g/mL}$  CRP (**Figure 20**). This appeared to improve outcomes, but flow issues prevented results from future experiments with this condition when attempting to lower the CRP concentration.

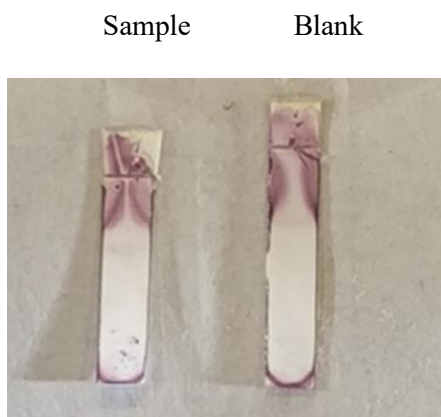


**Figure 18.** Results of half-strip assays with striped anti-CRP strips (aged 3 days) that were double-striped with antibody. CRP and secondary antibody concentrations of 50  $\mu\text{g/mL}$  and 10  $\mu\text{g/mL}$  were used. Signal in the sample and blank strips was comparable, but amplified compared to normal striping methods. In addition to the increase in background signal, flow issues were also observed, where liquid began to flow at a slower rate and pool at the site of application during testing. This is indicated by the purple residue on the test strip and caused some conditions to feature less than 3 replicates.

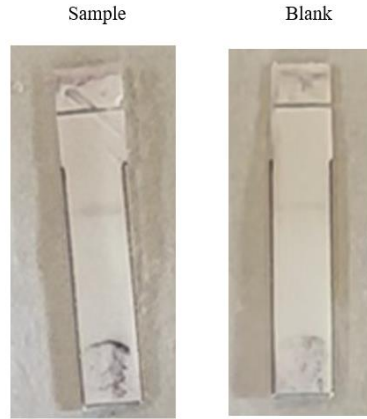


**Figure 19.** Results of half-strip assays with striped anti-CRP strips (aged 4 weeks) that had a sugar-salt solution coating antibody at the test line. CRP and secondary antibody concentrations of 10 ng/mL were used. Once again, the signal in the sample and blank strips was amplified compared to normal striping methods, but featured high background signal in the blank strips. Flow issues continued to present during testing.

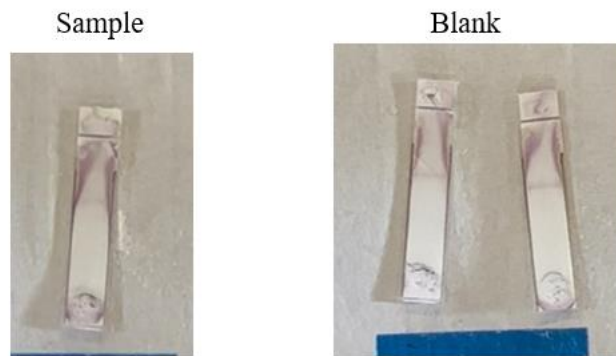


**Figure 20.** Results of half-strip assays with striped anti-CRP strips (aged 4 weeks) that had a sugar-salt solution coating antibody at the test line. CRP and secondary antibody concentrations of 1  $\mu$ g/mL and 10 ng/mL were used. Background signal was reduced, likely due to the lower concentration of biotinylated secondary antibody.

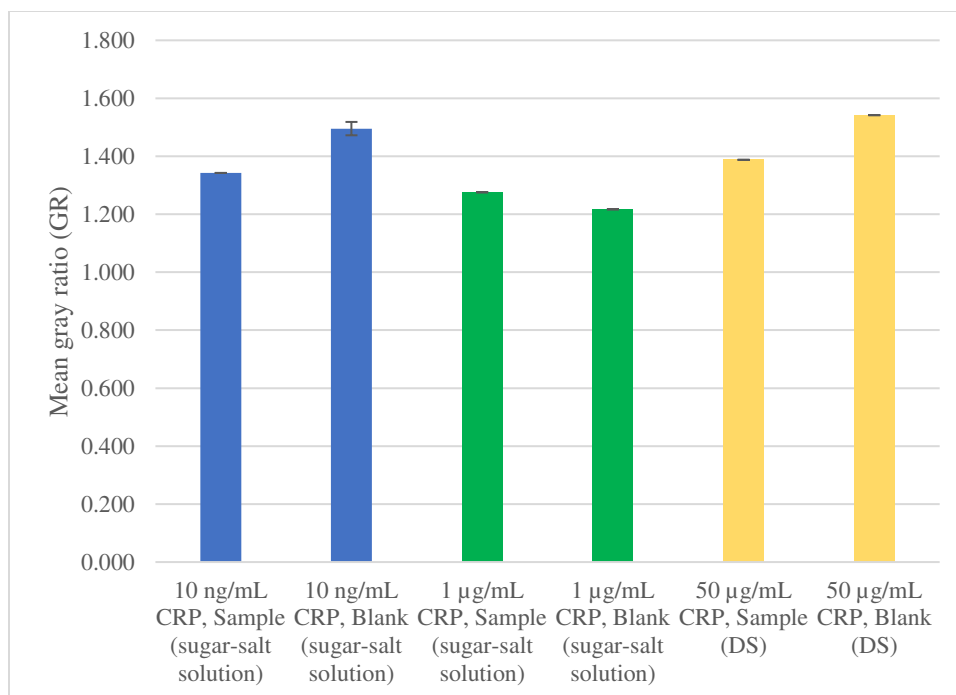


**Figure 21.** ImageJ results for alternative striping methods, including double-striped antibody (DS) and sugar-salt solution application.

While the end goal is not a test with CRP, experiments with this protein were useful in optimizing procedures involving nitrocellulose. From half-strip assays with spotted capture antibody, covalently-conjugated streptavidin-gold conjugate and a 30 nm gold nanoparticle size were selected due to more enhanced signal with the covalent conjugate and less non-specific binding with the 30 nm gold nanoparticles. For half-strip assays with striped antibody, 2 limitations of this research were realized. The first was that strips with striped antibody require immediate testing within the first 6 days or an aging period of 4 weeks before use. The second limitation is that striped nitrocellulose strips tend to flood, or stop wicking liquid through to the waste pad, during half-strip assays, though this was not an occurrence in every test strip. Regarding normal antibody striping techniques, concentrations of CRP down to 10 µg/mL produced signal. Double-striping antibody resulted in signal amplification, but background signal was also amplified with this condition. Strips with a sugar-salt solution coated over the capture

antibody produced encouraging results, with CRP concentrations down to 1  $\mu\text{g}/\text{mL}$  producing signal.

#### *Half-strip assays with striped anti-rbIFNT strips*

Half-strip assays were conducted in a similar manner using anti-rbIFNT strips, but spotting experiments were omitted in the interest of time and due to the increased experience in methodology gained through the CRP experiments. Another change was the type of nitrocellulose used. Previous experiments with CRP used an FF80 HP nitrocellulose membrane, which was initially selected due to the increased pore size and capillary flow rate. Increasingly poor flow characteristics in experiments prompted a switch in case it might be due a manufacturing defect. A nitrocellulose membrane from Vivid™, which is called Vivid-90 in this thesis, was used in experiments going forward. Though not identical, the pore size is similar enough to FF80 HP and would alter results much less than a switch to a membrane using a smaller pore size like FF120 HP (Nitrocellulose Membrane Selection for Lateral Flow - Fortis Life Sciences, n.d.).

Initial experiments were conducted with strips aged 6 weeks, as previous results demonstrated higher sensitivity with aged strips. A recombinant interferon-tau (rbIFNT) concentration of 10  $\mu\text{g}/\text{mL}$  produced a strong signal when paired with identical concentrations of biotinylated secondary antibody and streptavidin-conjugated horseradish peroxidase (HRP). However, strong background signal was also generated. Another test with 100 ng/mL rbIFNT (and a biotinylated secondary antibody concentration 100 times less than this) generated a readable signal, but this was also hard to distinguish from the background signal (**Figure 22**), with ImageJ results in **Figure 23**. In addition, some issues with flow persisted, as evidenced by the singular strip for the 100 ng/mL rbIFNT blank. These flow issues might be due to the half-

strip assay format, which requires a user to repeatedly add liquid instead of allowing the liquid to slowly absorb from a conjugate pad like in lateral flow assays (LFAs). With this knowledge and the demonstration of signal that scales with concentration added, the move to other test formats was pursued instead of further optimization with half-strip assays.



**Figure 22.** Results of half-strip assays with striped anti-rbIFNT strips that were aged 6 weeks. An enzymatic reaction was used to amplify signal at the test line. For 10 µg/mL rbIFNT, equivalent concentrations of biotinylated secondary antibody and streptavidin-conjugated HRP were used. For 100 ng/mL rbIFNT, 1 ng/ml of biotinylated secondary antibody was used. Background signal in blank strips was very high, but continuing flow issues prompted a switch to other point-of-care (POC) test formats.

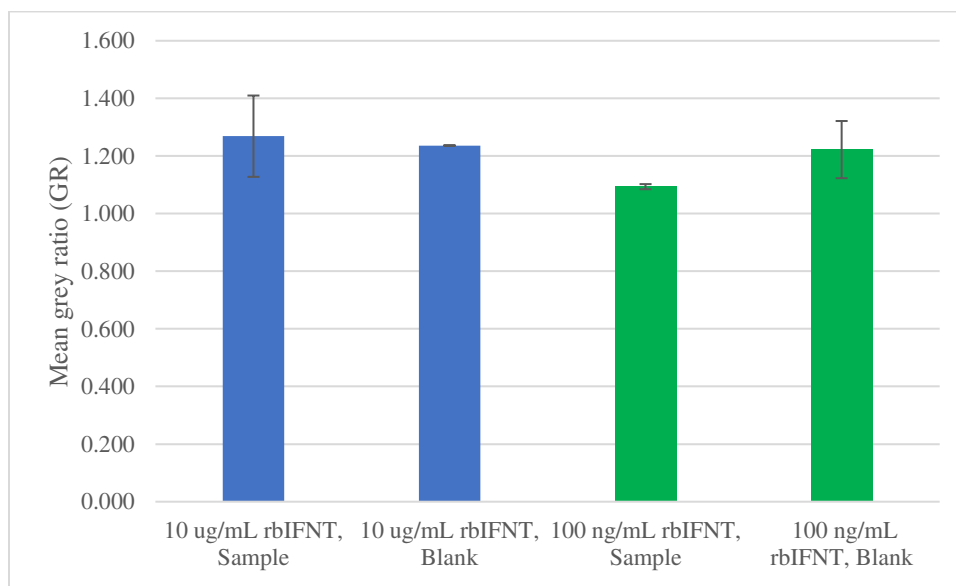


**Figure 23.** ImageJ results for all half-strip assays with anti-rbIFNT strips.

*Capillary-driven immunoassays (CaDI)*

Experimentation with CaDI was explored as an alternative to a lateral flow assay (LFA). Using strips aged 5 weeks, the first test utilized an rbIFNT concentration of 1  $\mu\text{g/mL}$  and biotinylated secondary antibody and streptavidin-conjugated HRP concentrations of 20 and 10  $\mu\text{g/mL}$ , respectively (**Figure 24**). This quickly led to the discovery of the main challenge associated with the full CaDI device: undesirable and irreproducible flow behavior within the microfluidic channel that depended strongly on the sample application method. As soon as sample was added and the microchannels filled with liquid, the TMB pad began to turn blue, exhibiting signs of the oxidation of TMB to its insoluble product. This was not ideal, as reagents were not supposed to mix inside the device. According to a supplementary information video from a recent publication (Clark et al., 2022), ideal flow involves clear liquid (sample or blank buffer) initially filling each side channel and entering the nitrocellulose strip. This is followed by flow of conjugate (or yellow dye) into the nitrocellulose strip. Clear liquid then flows into the nitrocellulose strip, followed by TMB (or blue dye). In this way, wash steps between reagents are established and reactions are restricted to the nitrocellulose strip.

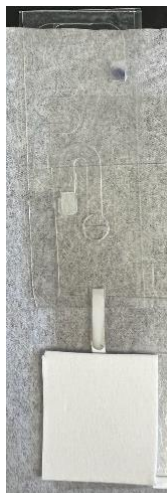


**Figure 24.** Initial tests with the capillary-driven immunoassay (CaDI) were conducted, with conjugate (secondary antibody labelled with HRP) and TMB pads to release reagents. The conjugate was bound using a biotin-streptavidin bond. Results demonstrated improper flow within the device. This was indicated by the formation of blue, oxidized TMB product in the TMB pad (upper right pad), which shows that reagents in the conjugate pad (lower left pad) flowed towards the TMB pad. Ideal flow within the CaDI involves no interactions of the conjugate and TMB within the microchannels – instead, reagents are sequentially delivered to the nitrocellulose membrane, with wash steps in between additions.

Dye-only experiments were conducted to improve sample application methodology to address flow issues within the device. This was conducted by adding yellow and blue dye to the conjugate and TMB pads, respectively, and adding 100  $\mu$ L of PBS to the device and observing for 15 minutes. Regions of the circular inlet were identified and targeted as the focus of the pipette tip (**Figure 25**). Ultimately, a solution was found by applying buffer at a moderate pace and moving the pipette tip slowly from region 1 to region 3, so that a droplet of liquid formed at the inlet (**Figure 26**). This allowed the device to pull liquid using capillary flow instead of moving liquid through the microchannels with the force of a pipette. The droplet likely formed due to the hydrophobic PET film making up region 3, which laid on top of the hydrophilic PET film making up region 1 and formed a vertical height difference constituting a step at region 2. In **Figure 25**, the mechanism of sequential reagent delivery was demonstrated by the different layers present in the waste pad, with layers further down the waste pad being delivered first.

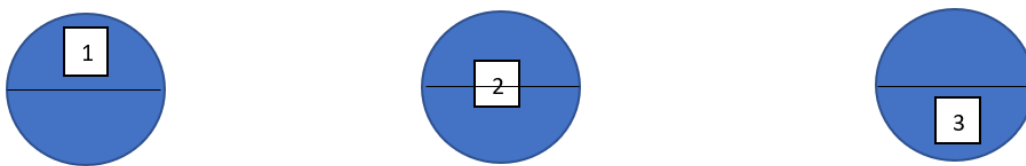


**Figure 25.** After the sample application methodology was narrowed down as the cause of improper flow within the device, several regions of the circular inlet were targeted for pipette application, as well as the speed at which sample was applied. This was conducted using dye-only experiments, where yellow dye is added to the conjugate pad and blue dye is added to the TMB pad. Region 1 features the hydrophilic PET film, while region 3 consists of the hydrophobic side of another layer of PET film. A vertical height difference is present at region 2. The optimized sample methodology included moving the pipette from region 1 to region 3 while dispensing sample at a moderate speed, so that a droplet of liquid formed at the inlet and allowed capillary flow to drive fluid flow within the device.

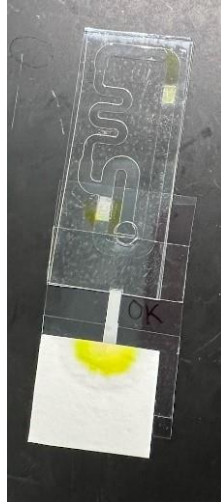


**Figure 26.** Using proper sample application methodology in a dye-only test, the mechanism of sequential delivery of reagents was demonstrated. This is evident in the waste pad, which shows the formation of different layers as the test proceeded.

Having improved the sample application methodology, experiments were conducted with reagents and dye to better observe the test progression. An rbIFNT concentration of 10  $\mu\text{g/mL}$  was tested with biotinylated secondary antibody (20  $\mu\text{g/mL}$ ) and streptavidin-conjugated HRP (30  $\mu\text{g/mL}$ ). Signal was produced in the sample strips and not in the blank strips (**Figure 27**), with ImageJ results shown in **Figure 28**. However, the validity of this signal was made questionable by the flow issues that still prevailed despite previous optimization, which was evident in the lack of yellow dye in the waste pads for over half of the strips. Due to the lack of reproducible signal stemming from flow issues, attention was switched to a hybrid lateral flow assay (LFA) utilizing enzyme signal amplification, with future optimization remaining for CaDI tests.

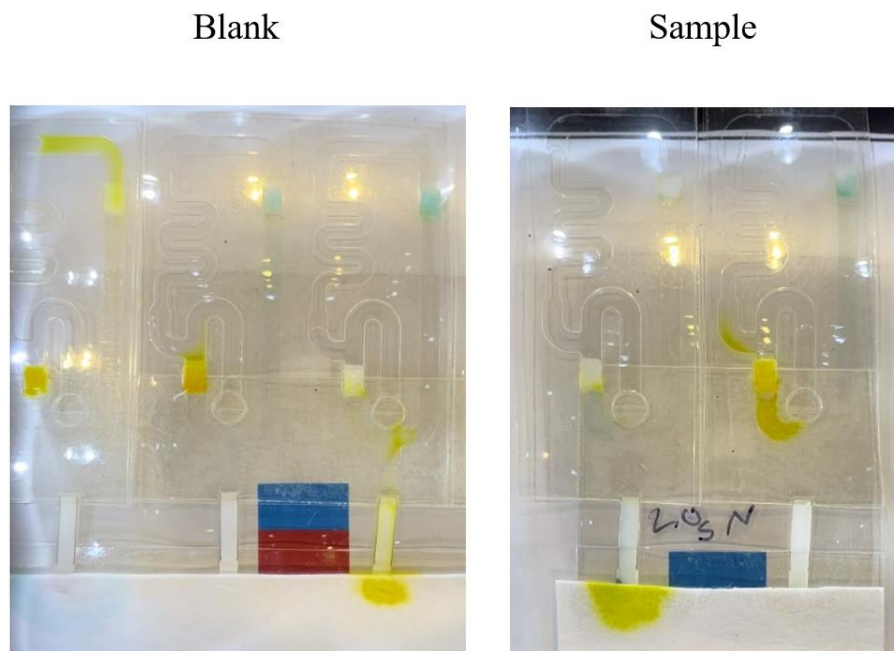


**Figure 27.** CaDI tests were conducted with 10  $\mu\text{g/mL}$  rbIFNT and 20  $\mu\text{g/mL}$  biotinylated secondary antibody. The conjugate was prepared with a 1:3 molar ratio of biotinylated secondary antibody to streptavidin-conjugated HRP, with reagents mixed and reacted at room temperature for 45 minutes before application to the conjugate pad. Despite sample application optimization, flow issues persisted, with over half of the devices not showing yellow dye in the waste pad. In addition, yellow dye is observed trapped in microchannels after the test was conducted. Potential signal was observed in the sample strips.

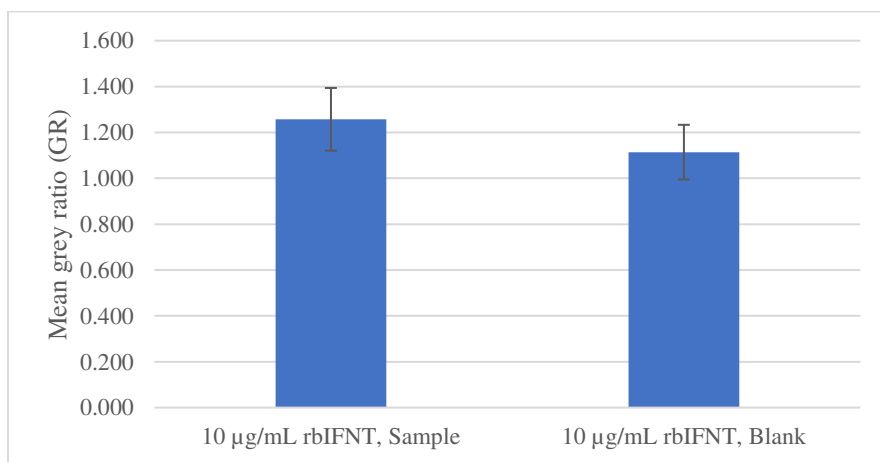


**Figure 28.** ImageJ results for CaDI tests.

### *Lateral flow assay format*

The first lateral flow assay (LFA) was tested with 10  $\mu\text{g/mL}$  rbIFNT and used aged conjugate pads made for CaDI devices (40  $\mu\text{g/mL}$  biotinylated secondary antibody, 60  $\mu\text{g/mL}$  streptavidin-conjugated HRP, aged 1.5 weeks) and a sample pad with the size of conjugate pads used in the LFA protocol. In this test, several methods of TMB application were tested, including layering a TMB pad after the conjugate pad, applying TMB to the sample pad, and applying TMB directly to the test line with a pipette. A wash step was not tested after TMB application. The only method that worked was the application of TMB directly at the test line (**Figure 29**), as the inclusion of a TMB pad resulted in an oxidation reaction in the TMB pad and adding TMB to the sample pad resulted in an oxidation reaction in the sample pad. The resulting signal from the strip allocated to direct TMB application was strong, and prompted a switch to working with lateral flow assays.



**Figure 29.** A lateral flow assay (LFA) was tested with 10  $\mu\text{g/mL}$  rbIFNT and a conjugate pad with 40  $\mu\text{g/mL}$  biotinylated secondary antibody. During testing, several methods of TMB application were used, including application at the sample pad and applying TMB directly to the test line with a pipette. Pictured is the result of applying TMB directly to the test line. Signal was present in the test line for the sample strip. The result of adding TMB to the sample pad was the formation of blue, oxidized TMB product in the sample pad.

The addition of a wash step after TMB addition presented a challenge with lateral flow assays: scaling pad protocols for larger conjugate and sample pads. For initial tests with this additional wash step, the test strips flooded and provided no useful results, although non-specific TMB that formed throughout the nitrocellulose strip was washed away after formation. Attempts to increase the volume of reagents added to pads, but not drying times, were not successful in fresh pads, as conjugate pads were wet during LFA assembly. After scaling pad protocols, tests were conducted with two different concentrations of biotinylated secondary antibody: 20  $\mu\text{g/mL}$  and 40  $\mu\text{g/mL}$  (with 30 and 60  $\mu\text{g/mL}$  streptavidin-conjugated HRP concentrations to achieve the 1:3 molar ratio). No signal was present in either test or blank strips, so a lightning kit conjugate was tested instead. This kit utilizes lysine residues or free reactive primary amines on antibodies to form a covalent bond between antibodies and HRP (*Lightning-Link® Antibody Conjugation Kits FAQs* | *Abcam*, n.d.).

Multiple concentrations of lightning kit conjugate were tested (10, 20, 30, 40, and 50  $\mu\text{g/mL}$ ). Results of these tests were not always clear, but began to yield signal in strips. Unfortunately, many of these signals were not located at the test line, but rather another region of the strip. A longer waiting period between steps (30 minutes vs. 15 minutes) was also tested, but resulted in most of the non-specific TMB remaining at the site of application (**Figure 30**).

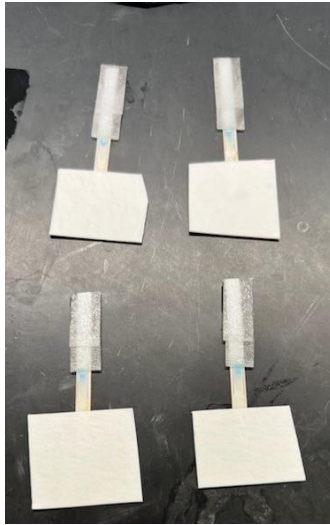


**Figure 30.** During testing, a waiting period of 15 minutes was applied before and after the first wash step. Modifying this to 30 minutes resulted in oxidized TMB product remaining at the site of application instead of being washed away with the final wash step. For this specific test, TMB was applied directly below the conjugate pad, where blue signal is present in all four strips.

20  $\mu\text{g/mL}$  of conjugate tested with 1  $\mu\text{g/mL}$  of rbIFNT in Tris buffer yielded signal near the test line (**Figure 31**). Tests with 30 and 40  $\mu\text{g/mL}$  of conjugate and 10  $\mu\text{g/mL}$  of rbIFNT revealed that pads aged 4 days performed better than fresh pads made the day of testing (**Figures 32 and 33**). The first strong evidence of signal at the test line occurred during a test with 50  $\mu\text{g/mL}$  of conjugate and 1  $\mu\text{g/mL}$  of rbIFNT in Tris buffer, with pads aged 7 days (**Figure 34**). However, signal was only present in blank strips, making this a strong background signal.

Sample Blank



**Figure 31.** LFAs were tested using a lightning kit conjugate instead of a conjugate bound with a biotin-streptavidin bond. Sample with 1  $\mu\text{g/mL}$  rbIFNT produced signal with 20  $\mu\text{g/mL}$  of conjugate, though signal was likely non-specific and is not located at the test line.

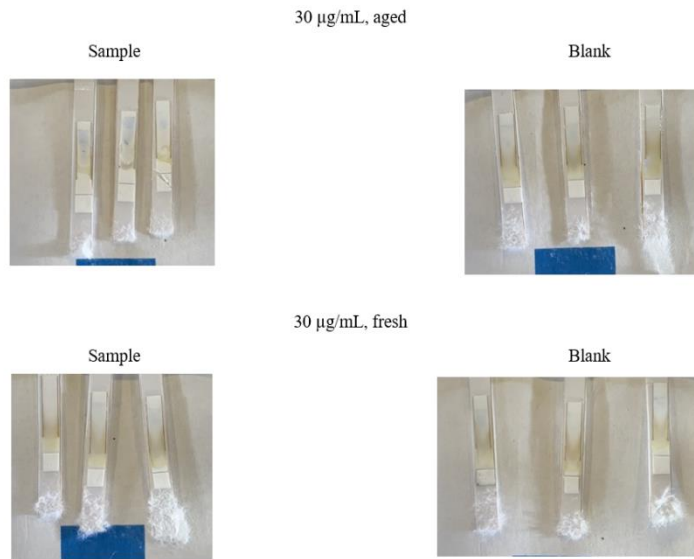


**Figure 32.** Lateral flow assays were tested with fresh and aged conjugate pads that were aged 4 days and had a conjugate concentration of 30  $\mu\text{g/mL}$ . A concentration of 1  $\mu\text{g/mL}$  rbIFNT was used. While resulting signal was non-specific, aged pads showed more activity than fresh conjugate pads.

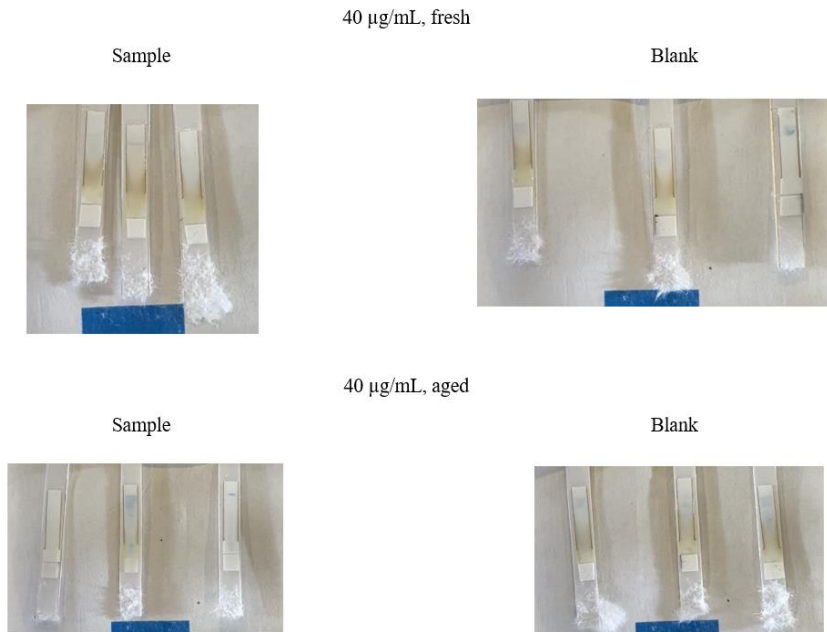


**Figure 33.** Lateral flow assays were tested with fresh and aged conjugate pads that were aged 4 days and had a conjugate concentration of 40  $\mu\text{g/mL}$ . A concentration of 1  $\mu\text{g/mL}$  rbIFNT was used. While resulting signal was non-specific, aged pads showed more activity than fresh conjugate pads.

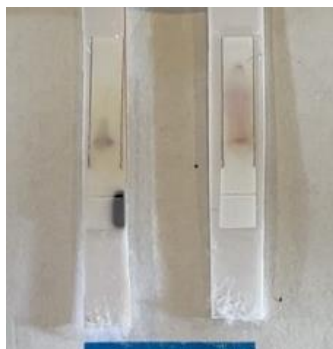


**Figure 34.** Lateral flow assays were tested with 1  $\mu\text{g/mL}$  of rbIFNT and 50  $\mu\text{g/mL}$  of conjugate, with conjugate pads aged 7 days. No signal was present in sample strips – however, strong background signal was present in blank strips, as pictured above.

## DISCUSSION

The goal of this research is to develop a point-of-care test for early pregnancy in dairy cows using interferon-tau (IFNT) as the biomarker. Steps towards that goal included investigation of different nitrocellulose protocols using C-reactive protein (CRP) to avoid wasting reagents. Half-strip assays were used during nitrocellulose methodology improvement to simplify operation. Later, a lateral flow assay (LFA) and capillary-driven immunoassay (CaDI) were explored in the development of the final test, with the goal of signal amplification utilizing the enzyme HRP and the substrate TMB and automated washing steps to remove weakly bound molecules.

From experiments using CRP and biotinylated secondary antibody conjugated with gold nanoparticles, the data suggests that particle size does have an impact on test signal. Particularly, 30 nm proved to be less sensitive, but more specific than 20 nm. Sensitivity refers to a test's ability to identify samples with the target analyte, while specificity refers to a test's ability to exclude samples with no target analyte (Boyce, 2017). Half-strip assay experiments with normal striping methods demonstrated signal for CRP concentrations down to 10  $\mu\text{g/mL}$ . As for alternative striping methods, double-striped antibody showed promise in increasing sensitivity, but requires optimization to avoid a major decrease in specificity from false positives and further testing with strips aged for several weeks. Strips with a sugar-salt solution coating over the capture antibody were more promising, with signal down to 1  $\mu\text{g/mL}$  CRP. However, this method requires extra work, as the second well in the BioSpot is used during striping. This could complicate procedures involving a control line, as antigen or antibody against the secondary antibody is usually placed in this well. Both normal antibody striping techniques and coating

sugar-salt solution over the capture antibody also produced signal at 10 ng/mL CRP, but these tests had such high background signal that it was likely only background signal was produced.

One major discovery of the CRP work was the required aging process for strips. Work in early days after strip production often resulted in strong signal that reduced quickly, only to return after 4 weeks of aging at room temperature (RT) in a low humidity environment. The hypothesis for this is that antibody striped onto nitrocellulose unfolds as it is deposited and takes several weeks to re-fold into a working conformation. Interestingly, the behavior leading to the aging process is not observed with spotted antibody, so it must be a product of forcing antibody through the wells in the BioSpot. This work focused on older strips, despite some decreasing signal, as it is difficult to stripe less than 10  $\mu$ L at a time and strips would age before they could all be tested in time. In a production scenario, older strips would still likely be favored due to the ability to sell strips for longer than just a few days. Optimization could also be done to see if this requirement goes away, although this observation is present in similar work (Samper et al., 2021).

Half-strip experiments have one operational weakness that makes transitioning to other testing formats difficult: strips often saturate quickly upon liquid addition, even though less than 100  $\mu$ L is added individually to each strip. Though half-strip assays are valuable for optimizing nitrocellulose protocols, they may not be ideal for accurately increasing sensitivity, as they favor a nitrocellulose membrane with a higher pore size and faster capillary-driven flow rate. Traditionally, a lower pore size and slower capillary flow rate is associated with better sensitivity, though specificity may also decrease with pore size (*Nitrocellulose Membrane Selection for Lateral Flow* - Fortis Life Sciences, n.d.). Ultimately, deciding on the type of the nitrocellulose

when doing half-strip experiments could cause issues down the road, although this was realized too late to implement into current work.

Tests with the capillary-driven immunoassay (CaDI) did not turn out as expected, but also brought up an important perspective for a point-of-care test. Flow issues due to sample application methodology were present, indicated by a TMB oxidation reaction occurring in the TMB pad and a lack of sequential reagent delivery visualized during dye-only experiments. Even after optimization of this methodology, flow issues were still present during experiments using reagents and dye, though signal was obtained in several strips. The flow issues raise a good question: could a dairy farmer perform this test accurately? Even with detailed instructions, flow issues could be present until the farmer gained more experience with the test. Future work involving changes in inlet geometry may improve this, but as this is not the focus of this thesis, a simpler and more reproducible test format was pursued in the form of a hybrid lateral flow assay (LFA).

Lateral flow assays using HRP and TMB presented some challenges, as the TMB could not be added directly to the sample pad. Application of TMB directly at the test line worked in an initial test, although subsequent tests showed that optimization is needed to obtain signal in the test line again. Though clear signal in the test line was not obtained, tests with aged vs. fresh pads showed that aged pads performed better, with more of a reaction in the strips. Clear signal at the test line was again obtained, but as background signal with a lightning kit conjugate concentration of 50  $\mu\text{g/mL}$ . Once again, this set-up could be a bit complex for a dairy farmer, and takes more time/steps than an LFA utilizing gold nanoparticles as the detection label. Future work utilizing gold nanoparticles conjugated directly with a lightning kit would be valuable in attempting to achieve the same level of sensitivity, especially with the issues faced in the current

system. Regarding the current system, more work could be done to try to add TMB to the sample pad, as has been reported in some previous literature (Samsonova et al., 2015; Zhang et al., 2019). Overall, further optimization of this test is required before consideration of a market-level product.

## CONCLUSION

This research was performed with the intent to develop a point-of-care test for early pregnancy in dairy cows using interferon-tau (IFNT) as the biomarker. Optimization of nitrocellulose protocols with C-reactive protein (CRP) and gold nanoparticles as the detection particle was first performed, followed by experimentation with a capillary driven immunoassay (CaDI) and a hybrid lateral flow assay utilizing TMB and HRP to produce an amplified signal at the test line.

From half-strip assays with spotted anti-CRP strips, 30 nm gold nanoparticles were chosen over 20 nm gold nanoparticles due to the reduction of non-specific binding. Covalently-conjugated streptavidin-gold conjugate was found to produce much stronger signal than passively-conjugated conjugate from the same company. Half-strip assays with striped anti-CRP strips produced signal with 10  $\mu\text{g/mL}$  with normal striping methods and 1  $\mu\text{g/mL}$  with the addition of a sugar-salt coating over the capture antibody at the test line. Signal at the ng/mL level was observed, with 10 ng/mL of CRP producing a signal in each condition, but background signal was prevalent at these low concentrations. Double-striping antibody onto the test line showed potential in increasing sensitivity, but also an increase in background signal and a need for more testing with this condition. Two major limitations of this work were also discovered during striped anti-CRP half-strip assays: a required aging process after strip production spanning at least 4 weeks, and a tendency of strips to flood during half-strip assays. Initial tests with striped anti-CRP half strips aged 6 days or longer revealed that no signal was produced in sample or blank strips, even with CRP concentrations of 100  $\mu\text{g/mL}$ . After further testing with strips aged 2-4 weeks, it was demonstrated that 4 weeks is the earliest strips can be tested in order to obtain desirable results. Tests with 2 different blocking protocols, the first with much

shorter drying steps, showed that capture antibody stability and overall flow characteristics were improved with the second blocking protocol, though flow issues were still present.

Half-strip assays with anti-rbIFNT strips demonstrated signal with 100 ng/mL, though the background signal was equally strong. Tests with capillary-driven immunoassays (CaDI) showed potential, though a significant user issue was revealed: based on the methodology used to apply sample, improper flow within the device could occur. Tests using only dye were conducted to improve sample application methodology, and the use of dye was continued afterwards with reagents to continue to better monitor the flow of reagents. Ultimately, the dye-only experiments helped to identify an optimal method for sample application, but experiments with reagent and dye showed continuing issues with improper flow and a need for the user to have expertise in applying sample to the device, which is not ideal for a point-of-care (POC) test.

Tests with hybrid lateral flow assays also showed potential, but with the need for much future work. Signal was obtained by introducing a wash step after sample and TMB application and applying TMB directly to the test line with a pipette, with 10  $\mu\text{g/mL}$  rbIFNT producing signal. However, this proved to be very difficult to reproduce, and the only other signal present was strong background signal in LFAs using 50  $\mu\text{g/mL}$  of lightning kit conjugate. Despite the lack of signal in the test line, non-specific signal allowed other observations to be made, such as the improved performance of aged conjugate pads versus fresh conjugate pads. This was indicated by the formation of insoluble oxidized TMB product in the nitrocellulose strips during testing, which showed that the conjugate in aged pads was more active than conjugate in fresh pads. Replacing the 15 min wait period with a 30 min wait period was also ruled out, as this resulted in the TMB remaining at the site of application with no removal of non-specific product with a wash step.

Regarding future work, several approaches could be taken by future researchers. First, the type of nitrocellulose used in lateral flow assays and capillary-driven immunoassays could use further optimization. While nitrocellulose with a larger pore size and faster capillary flow rate (FF80HP, Vivid-90) provided a good medium for half-strip assays, a smaller pore size and slower capillary flow rate (FF120 HP) could contribute to increased sensitivity. Unlike in half-strip assays, nitrocellulose strips did not flood with these tests, so the slower capillary flow rate would likely not be problematic.

While results with CaDI were not optimal, this device has great potential due to signal amplification from the enzymatic reaction and automated washing steps, which can reduce non-specific binding. A different inlet geometry could be explored to reduce the expertise needed for proper sample application. For lateral flow assays, the hybrid LFA utilizing an enzymatic reaction requires more work, as signal is currently irreproducible and the test requires multiple steps. Blocking protocols for the sample pad or a change in substrate solution could be explored for the potential addition of substrate (TMB) at the sample pad instead of the test line. Using gold nanoparticles as the detection particle could also be explored, as this would reduce the number of steps during the test. While tests were conducted with gold nanoparticles during CRP half-strip assays, these utilized a biotin-streptavidin bond to link secondary antibody to gold nanoparticles. Conjugating the gold nanoparticles directly to the secondary antibody using a lightning kit could produce better results, with a potential reduction in false positive signal.

## REFERENCES

- Abbitt, B., Ball, L., Kitto, G. P., Sitzman, C. G., Wilgenburg, B., Raim, L. W., & Seidel, G. E. (1978). Effect of three methods of palpation for pregnancy diagnosis per rectum on embryonic and fetal attrition in cows. *Journal of the American Veterinary Medical Association*, *173*(8), 973–977.
- Albaaj, A., Durocher, J., LeBlanc, S. J., & Dufour, S. (2022). Meta-analysis of the incidence of pregnancy losses in dairy cows at different stages to 90 days of gestation. *JDS Communications*, *4*(2), 144–148. <https://doi.org/10.3168/jdsc.2022-0278>
- Alertys OnFarm ruminant pregnancy test—IDEXX US*. (n.d.). Retrieved June 12, 2023, from <https://www.idexx.com/en/livestock/livestock-tests/ruminant-tests/idexx-pregnancy-tests/alertys-onfarm-ruminant-pregnancy-test/>
- Amini, M., Pourmand, M. R., Faridi-Majidi, R., Heiat, M., Mohammad Nezhady, M. A., Safari, M., Noorbakhsh, F., & Baharifar, H. (2020). Optimising effective parameters to improve performance quality in lateral flow immunoassay for detection of PBP2a in methicillin-resistant *Staphylococcus aureus* (MRSA). *Journal of Experimental Nanoscience*, *15*(1), 266–279. <https://doi.org/10.1080/17458080.2020.1775197>
- Analyze Menu*. (n.d.). Retrieved June 15, 2023, from <https://imagej.nih.gov/nih-image/manual/menus/analyze.html>
- Bazer, F. W., Burghardt, R. C., Johnson, G. A., Spencer, T. E., & Wu, G. (2018). Mechanisms for the establishment and maintenance of pregnancy: Synergies from scientific collaborations†. *Biology of Reproduction*, *99*(1), 225–241. <https://doi.org/10.1093/biolre/i0y047>

- BioPRYN for Dairy Cattle—The blood pregnancy test. (n.d.). *BioPRYN*. Retrieved June 12, 2023, from <https://biopryn.com/biopryn-dairy/>
- Bovine Interferon Tau (IFN $\tau$ ) ELISA Kit, Cat#EKU09093*. (n.d.). Biomatik. Retrieved June 12, 2023, from <https://www.biomatik.com/elisa-kits/bovine-interferon-tau-ifnt-elisa-kit-cat-eku09093/>
- Boyce, D. (2017). Chapter 17—Evaluation of Medical Laboratory Tests. In J. D. Placzek & D. A. Boyce (Eds.), *Orthopaedic Physical Therapy Secrets (Third Edition)* (pp. 125–134). Elsevier. <https://doi.org/10.1016/B978-0-323-28683-1.00017-5>
- Cabrera, V. E. (2014). Economics of fertility in high-yielding dairy cows on confined TMR systems. *Animal: An International Journal of Animal Bioscience*, *8 Suppl 1*, 211–221. <https://doi.org/10.1017/S1751731114000512>
- Calabria, D., Calabretta, M. M., Zangheri, M., Marchegiani, E., Trozzi, I., Guardigli, M., Michelini, E., Di Nardo, F., Anfossi, L., Baggiani, C., & Mirasoli, M. (2021). Recent Advancements in Enzyme-Based Lateral Flow Immunoassays. *Sensors (Basel, Switzerland)*, *21*(10), 3358. <https://doi.org/10.3390/s21103358>
- Carrell, C., Jang, I., Link, J., Terry, J. S., Call, Z., Panraksa, Y., Chailapakul, O., Dandy, D. S., Geiss, B. J., & Henry, C. S. (2023). Capillary driven microfluidic sequential flow device for point-of-need ELISA: COVID-19 serology testing. *Analytical Methods*, *15*(22), 2721–2728. <https://doi.org/10.1039/D3AY00225J>
- Chamorro-Garcia, A., de la Escosura-Muñiz, A., Espinoza-Castañeda, M., Rodriguez-Hernandez, C. J., de Torres, C., & Merkoçi, A. (2016). Detection of parathyroid hormone-like hormone in cancer cell cultures by gold nanoparticle-based lateral flow immunoassays.

*Nanomedicine: Nanotechnology, Biology and Medicine*, 12(1), 53–61.

<https://doi.org/10.1016/j.nano.2015.09.012>

Clark, K. M., Schenkel, M. S., Pittman, T. W., Samper, I. C., Anderson, L. B. R., Khamcharoen, W., Elmegerhi, S., Perera, R., Siangproh, W., Kennan, A. J., Geiss, B. J., Dandy, D. S., & Henry, C. S. (2022). Electrochemical Capillary Driven Immunoassay for Detection of SARS-CoV-2. *ACS Measurement Science Au*, 2(6), 584–594.

<https://doi.org/10.1021/acsmeasuresciau.2c00037>

*Covalent Conjugation of Proteins to Carboxylated Gold Nanoparticles*. (n.d.). Cytodiagnostics Inc. Retrieved June 20, 2023, from <https://www.cytodiagnostics.com/pages/covalent-conjugation-of-proteins-to-carboxylated-gold-nanoparticles>

Hansen, T. R., Sinedino, L. D. P., & Spencer, T. E. (2017). Paracrine and endocrine actions of interferon tau (IFNT). *Reproduction*, 154(5), F45–F59. <https://doi.org/10.1530/REP-17-0315>

Humblot, F., Camous, S., Martal, J., Charlery, J., Jeanguyot, N., Thibier, M., & Sasser, R. G. (1988). Pregnancy-specific protein B, progesterone concentrations and embryonic mortality during early pregnancy in dairy cows. *Journal of Reproduction and Fertility*, 83(1), 215–223. <https://doi.org/10.1530/jrf.0.0830215>

Kawaguchi, T., Cho, D., Hayashi, M., Tsukiyama, T., Kimura, K., Matsuyama, S., Minami, N., Yamada, M., & Imai, H. (2016). Derivation of Induced Trophoblast Cell Lines in Cattle by Doxycycline-Inducible piggyBac Vectors. *PLOS ONE*, 11(12), e0167550.

<https://doi.org/10.1371/journal.pone.0167550>

- Kiracofe, G. H., Wright, J. M., Schalles, R. R., Ruder, C. A., Parish, S., & Sasser, R. G. (1993). Pregnancy-specific protein B in serum of postpartum beef cows. *Journal of Animal Science*, *71*(8), 2199–2205. <https://doi.org/10.2527/1993.7182199x>
- Latex agglutination test: MedlinePlus Medical Encyclopedia*. (n.d.). Retrieved June 12, 2023, from <https://medlineplus.gov/ency/article/003334.htm>
- Lightning-Link® Antibody conjugation kits FAQs | Abcam*. (n.d.). Retrieved July 11, 2023, from <https://www.abcam.com/help/antibody-conjugation-kits---frequently-asked-questions-faqs>
- Mahmoudi, T., de la Guardia, M., & Baradaran, B. (2020). Lateral flow assays towards point-of-care cancer detection: A review of current progress and future trends. *TrAC Trends in Analytical Chemistry*, *125*, 115842. <https://doi.org/10.1016/j.trac.2020.115842>
- Medicine, C. for V. (2021). The Cattle Estrous Cycle and FDA-Approved Animal Drugs to Control and Synchronize Estrus—A Resource for Producers. *FDA*. <https://www.fda.gov/animal-veterinary/product-safety-information/cattle-estrous-cycle-and-fda-approved-animal-drugs-control-and-synchronize-estrus-resource-producers>
- Meidan, R., & Basavaraja, R. (2022). Interferon-Tau regulates a plethora of functions in the corpus luteum. *Domestic Animal Endocrinology*, *78*, 106671. <https://doi.org/10.1016/j.domaniend.2021.106671>
- Niswender, G. D., Juengel, J. L., Silva, P. J., Rollyson, M. K., & McIntush, E. W. (2000). Mechanisms Controlling the Function and Life Span of the Corpus Luteum. *Physiological Reviews*, *80*(1), 1–29. <https://doi.org/10.1152/physrev.2000.80.1.1>
- Nitrocellulose Membrane Selection for Lateral Flow—Fortis Life Sciences*. (n.d.). Retrieved June 14, 2023, from <https://www.fortislife.com/nitrocellulose-membrane-selection>

- Nsamela, A. (2020). Microfluidics for point-of-care diagnostic devices: A review. *Elveflow*.  
<https://www.elveflow.com/microfluidic-reviews/general-microfluidics/microfluidics-for-point-of-care-diagnostic-devices-a-review/>
- O'Farrell, B. (2008). Evolution in Lateral Flow–Based Immunoassay Systems. *Lateral Flow Immunoassay*, 1–33. [https://doi.org/10.1007/978-1-59745-240-3\\_1](https://doi.org/10.1007/978-1-59745-240-3_1)
- Parolo, C., de la Escosura-Muñiz, A., & Merkoçi, A. (2013). Enhanced lateral flow immunoassay using gold nanoparticles loaded with enzymes. *Biosensors and Bioelectronics*, 40(1), 412–416. <https://doi.org/10.1016/j.bios.2012.06.049>
- Plotz, C. M., & Singer, J. M. (1956). The latex fixation test. I. Application to the serologic diagnosis of rheumatoid arthritis. *The American Journal of Medicine*, 21(6), 888–892.
- Prostaglandin Based Estrus Synchronization in Postpartum Dairy Cows: An Update*. (n.d.). Retrieved June 12, 2023, from <http://www.jarvm.com/articles/Vol1Iss1/LOPEZDJVM.htm>
- Sajid, M., Kawde, A.-N., & Daud, M. (2015). Designs, formats and applications of lateral flow assay: A literature review. *Journal of Saudi Chemical Society*, 19(6), 689–705.  
<https://doi.org/10.1016/j.jscs.2014.09.001>
- Samper, I. C., Sánchez-Cano, A., Khamcharoen, W., Jang, I., Siangproh, W., Baldrich, E., Geiss, B. J., Dandy, D. S., & Henry, C. S. (2021). Electrochemical Capillary-Flow Immunoassay for Detecting Anti-SARS-CoV-2 Nucleocapsid Protein Antibodies at the Point of Care. *ACS Sensors*, 6(11), 4067–4075. <https://doi.org/10.1021/acssensors.1c01527>
- Samsonova, J. V., Safronova, V. A., & Osipov, A. P. (2015). Pretreatment-free lateral flow enzyme immunoassay for progesterone detection in whole cows' milk. *Talanta*, 132, 685–689. <https://doi.org/10.1016/j.talanta.2014.10.043>

- Sasser, R. G., Crock, J., & Ruder-Montgomery, C. A. (1989). Characteristics of pregnancy-specific protein B in cattle. *Journal of Reproduction and Fertility. Supplement*, 37, 109–113.
- Sasser, R. G., Ruder, C. A., Ivani, K. A., Butler, J. E., & Hamilton, W. C. (1986). Detection of pregnancy by radioimmunoassay of a novel pregnancy-specific protein in serum of cows and a profile of serum concentrations during gestation. *Biology of Reproduction*, 35(4), 936–942. <https://doi.org/10.1095/biolreprod35.4.936>
- Shi, F., Zhao, Y., Sun, Y., & Chen, C. (2020). Development and application of a colloidal carbon test strip for the detection of antibodies against *Mycoplasma bovis*. *World Journal of Microbiology & Biotechnology*, 36(10), 157. <https://doi.org/10.1007/s11274-020-02930-2>
- Spencer, T. E., Forde, N., & Lonergan, P. (2016). The role of progesterone and conceptus-derived factors in uterine biology during early pregnancy in ruminants1. *Journal of Dairy Science*, 99(7), 5941–5950. <https://doi.org/10.3168/jds.2015-10070>
- Szenci, O., Beckers, J. F., Humblot, P., Sulon, J., Sasser, G., Taverne, M. A., Varga, J., Baltusen, R., & Schekk, G. (1998). Comparison of ultrasonography, bovine pregnancy-specific protein B, and bovine pregnancy-associated glycoprotein 1 tests for pregnancy detection in dairy cows. *Theriogenology*, 50(1), 77–88. [https://doi.org/10.1016/s0093-691x\(98\)00115-0](https://doi.org/10.1016/s0093-691x(98)00115-0)
- Tabatabaei, M. S., & Ahmed, M. (2022). Enzyme-Linked Immunosorbent Assay (ELISA). *Methods in Molecular Biology (Clifton, N.J.)*, 2508, 115–134. [https://doi.org/10.1007/978-1-0716-2376-3\\_10](https://doi.org/10.1007/978-1-0716-2376-3_10)

*The GENEX Blog: Dairy Synchronization: A Learning Experience—Part 1.* (n.d.). Retrieved June 11, 2023, from <http://crinetsupport.blogspot.com/2015/07/dairy-synchronization-learning.html>

Vaillancourt, D., Bierschwal, C. J., Ogwu, D., Elmore, R. G., Martin, C. E., Sharp, A. J., & Youngquist, R. S. (1979). Correlation between pregnancy diagnosis by membrane slip and embryonic mortality. *Journal of the American Veterinary Medical Association*, *175*(5), 466–468.

Yang, S.-M., Lv, S., Zhang, W., & Cui, Y. (2022). Microfluidic Point-of-Care (POC) Devices in Early Diagnosis: A Review of Opportunities and Challenges. *Sensors (Basel, Switzerland)*, *22*(4), 1620. <https://doi.org/10.3390/s22041620>

Yin, H.-Y., Li, Y.-T., Tsai, W.-C., Dai, H.-Y., & Wen, H.-W. (2022). An immunochromatographic assay utilizing magnetic nanoparticles to detect major peanut allergen Ara h 1 in processed foods. *Food Chemistry*, *375*, 131844. <https://doi.org/10.1016/j.foodchem.2021.131844>

Zhang, J., Gui, X., Zheng, Q., Chen, Y., Ge, S., Zhang, J., & Xia, N. (2019). An HRP-labeled lateral flow immunoassay for rapid simultaneous detection and differentiation of influenza A and B viruses. *Journal of Medical Virology*, *91*(3), 503–507. <https://doi.org/10.1002/jmv.25322>

APPENDICES

**Table 1.** Image J values for all work with striped anti-CRP half strips, excluding double-striped and sugar-salt solution-coated half strips.

<i>Figure #</i>	<i>Condition</i>	<i>Mean T</i>	<i>Mean B</i>	<i>Mean Grey Ratio (GR)</i>	<i>St. Dev. Of Mean GR</i>	
7	1000 µg/mL CRP, Covalent Conjugation	51.875	35.065	1.479	0.168	
		54.656	32.221	1.696		
		54.095	39.631	1.365		
	<b>Average</b>	<b>53.542</b>	<b>35.639</b>	<b>1.502</b>		
	1000 µg/mL CRP, Passive Conjugation	80.595	78.919	1.021		0.047
87.957		82.794	1.062			
73.341		75.722	0.969			
<b>Average</b>	<b>80.631</b>	<b>79.145</b>	<b>1.019</b>			
8	100 µg/mL CRP	87.000	64.260	1.354	0.075	
		90.185	69.184	1.304		
		84.340	69.928	1.206		
	<b>Average</b>	<b>87.175</b>	<b>67.791</b>	<b>1.286</b>		
	10 µg/mL CRP	73.149	64.033	1.142		0.043
		67.602	57.002	1.186		
		72.250	65.723	1.099		
	<b>Average</b>	<b>71.000</b>	<b>62.253</b>	<b>1.141</b>		
	Blank	69.636	55.447	1.256	0.086	
		78.164	57.994	1.348		
76.546		65.132	1.175			
<b>Average</b>	<b>74.782</b>	<b>59.524</b>	<b>1.256</b>			
9	10 µg/mL CRP	79.067	62.782	1.259		0.034
		96.691	81.141	1.192		
		77.811	63.038	1.234		
	<b>Average</b>	<b>84.523</b>	<b>68.987</b>	<b>1.225</b>		
	Blank	61.514	58.946	1.044	0.017	
61.387		57.174	1.074			
66.762		63.791	1.047			
<b>Average</b>	<b>63.221</b>	<b>59.970</b>	<b>1.054</b>			
11	1000 µg/mL CRP (no sodium azide)	73.635	51.478	1.430		0.102
		86.134	66.941	1.287		
		<b>Average</b>	<b>79.885</b>	<b>59.210</b>	<b>1.349</b>	
	Blank	51.441	44.062	1.167	0.094	
		57.465	55.532	1.035		
<b>Average</b>	<b>54.453</b>	<b>49.797</b>	<b>1.093</b>			
100 µg/mL CRP (no sodium azide)	73.512	52.715	1.395	0.190		

12		80.800	71.795	1.125	
	<b>Average</b>	<b>77.156</b>	<b>62.255</b>	<b>1.239</b>	
	Blank	77.559	62.237	1.246	0.134
13		85.842	85.919	0.999	
		71.486	69.347	1.031	
	<b>Average</b>	<b>78.296</b>	<b>72.501</b>	<b>1.080</b>	
	100 µg/mL CRP	61.003	48.556	1.256	0.097
		63.781	57.003	1.119	
	<b>Average</b>	<b>62.392</b>	<b>52.780</b>	<b>1.182</b>	
14	Blank	65.722	51.677	1.272	0.045
		64.836	53.398	1.214	
		67.783	57.291	1.183	
	<b>Average</b>	<b>66.114</b>	<b>54.122</b>	<b>1.222</b>	
	241 µg/mL CRP, Sample	99.358	62.062	1.601	0.082
		93.340	62.850	1.485	
	<b>Average</b>	<b>96.349</b>	<b>62.456</b>	<b>1.543</b>	
	241 µg/mL CRP, Blank	67.959	49.799	1.365	0.133
		75.618	61.192	1.236	
		69.882	63.566	1.099	
15	<b>Average</b>	<b>71.153</b>	<b>58.186</b>	<b>1.223</b>	
	100 µg/mL CRP, Sample	96.329	49.121	1.961	0.319
		94.059	62.279	1.510	
	<b>Average</b>	<b>95.194</b>	<b>55.700</b>	<b>1.709</b>	
	100 µg/mL CRP, Blank	58.264	45.280	1.287	0.114
		68.184	64.091	1.064	
		61.338	54.139	1.133	
	<b>Average</b>	<b>62.595</b>	<b>54.503</b>	<b>1.148</b>	
	20 µg/mL CRP, Sample	67.717	63.087	1.073	0.178
		60.010	42.030	1.428	
16		54.570	42.907	1.272	
	<b>Average</b>	<b>60.766</b>	<b>49.341</b>	<b>1.232</b>	
	20 µg/mL CRP, Blank	50.684	41.067	1.234	0.120
		51.403	42.906	1.198	
		66.034	65.301	1.011	
	<b>Average</b>	<b>56.040</b>	<b>49.758</b>	<b>1.126</b>	
	10 µg/mL CRP, Blank	72.356	60.497	1.196	0.025
		70.449	60.729	1.160	
	<b>Average</b>	<b>71.403</b>	<b>60.613</b>	<b>1.178</b>	
	10 µg/mL CRP, Sample	<b>78.649</b>	<b>61.804</b>	<b>1.273</b>	N/A
16	10 ng/mL CRP, Sample	57.954	54.267	1.068	0.080
		59.646	54.019	1.104	
		42.998	35.235	1.220	
	<b>Average</b>	<b>53.533</b>	<b>47.840</b>	<b>1.119</b>	
	Blank	64.278	60.336	1.065	0.160

	61.815	58.243	1.061
	46.311	34.570	1.340
<b>Average</b>	<b>57.468</b>	<b>51.050</b>	<b>1.126</b>

**Table 2.** Image J values for double-striped (DS) anti-CRP half strips.

<i>Figure #</i>	<i>Condition</i>	<i>Mean T</i>	<i>Mean B</i>	<i>Mean Grey Ratio (GR)</i>	<i>St. Dev. Of Mean GR</i>
18	50 µg/mL CRP	<b>58.277</b>	<b>41.994</b>	<b>1.388</b>	N/A
	Blank	<b>88.831</b>	<b>57.614</b>	<b>1.542</b>	N/A

**Table 3.** Image J values for anti-CRP half strips with a sugar-salt solution coating the capture antibody.

<i>Figure #</i>	<i>Condition</i>	<i>Mean T</i>	<i>Mean B</i>	<i>Mean Grey Ratio (GR)</i>	<i>St. Dev. Of Mean GR</i>
19	10 ng/mL CRP, Sample	<b>86.976</b>	<b>64.789</b>	<b>1.342</b>	N/A
	10 ng/mL CRP, Blank	76.807	47.571	1.615	0.023
		77.552	49.022	1.582	
	<b>Average</b>	<b>80.445</b>	<b>53.794</b>	<b>1.495</b>	
20	1 µg/mL CRP, Sample	<b>70.490</b>	<b>55.252</b>	<b>1.276</b>	N/A
	1 µg/mL CRP, Blank	<b>70.154</b>	<b>57.639</b>	<b>1.217</b>	N/A

**Table 4.** Image J values for anti-rbIFNT half strips.

<i>Figure #</i>	<i>Condition</i>	<i>Mean T</i>	<i>Mean B</i>	<i>Mean Grey Ratio (GR)</i>	<i>St. Dev. Of Mean GR</i>
22	10 ug/mL rbIFNT, Sample	79.987	58.361	1.371	0.141
		78.213	57.924	1.350	
		78.317	70.141	1.117	
	<b>Average</b>	<b>78.839</b>	<b>62.142</b>	<b>1.269</b>	
	10 ug/mL rbIFNT, Blank	<b>66.685</b>	<b>53.939</b>	<b>1.236</b>	N/A
	100 ng/mL rbIFNT, Sample	73.923	68.006	1.087	0.009
		82.358	74.903	1.100	
	<b>Average</b>	<b>78.141</b>	<b>71.455</b>	<b>1.094</b>	

100 ng/mL	72.139	59.263	1.217	0.099
rbIFNT, Blank	61.526	45.981	1.338	
	71.030	62.242	1.141	
<b>Average</b>	<b>68.232</b>	<b>55.829</b>	<b>1.222</b>	

**Table 5.** ImageJ values for CaDI tests.

<i>Figure #</i>	<i>Condition</i>	<i>Mean T</i>	<i>Mean B</i>	<i>Mean Grey Ratio (GR)</i>	<i>St. Dev. Of Mean GR</i>
27	10 µg/mL rbIFNT, Sample	39.361	28.368	1.388	0.137
		69.894	58.533	1.194	
	<b>Average</b>	<b>54.628</b>	<b>43.451</b>	<b>1.257</b>	
	10 µg/mL rbIFNT, Blank	57.777	48.078	1.202	
		53.790	52.064	1.033	
	<b>Average</b>	<b>55.784</b>	<b>50.071</b>	<b>1.114</b>	